CHAPTER 2

The Mathematics of Chemotaxis

M.A. Herrero

Departamento de Matemática Aplicada, Facultad de CC. Matemáticas,
Universidad Complutense de Madrid, Avda. Complutense s/n, 28040 Madrid, Spain
E-mail: Miguel_Herrero@mat.ucm.es

Contents

Abstract

This chapter provides a description of some of the mathematical approaches that have been developed to account for quantitative and qualitative aspects of chemotaxis. This last is an important biological property, consisting in motion of cells induced by chemical substances, which is known to occur in a large number of situations, both homeostatic and pathological. Particular attention will be paid to the limits on a cell's capability to measure external cues on the one hand, and to provide an overall description of aggregation models for the slime mold *Dictyostelium discoideum* on the other.

HANDBOOK OF DIFFERENTIAL EQUATIONS
Evolutionary Equations, volume 3
Edited by C.M. Dafermos and E. Feireisl

1. Introduction: What is chemotaxis?

Chemotaxis is a technical term which is commonly used to describe the motion of cells induced by chemical substances, either to navigate toward the source of those, or else to escape away from them. This scientific concept was formulated as a hypothesis by Ramón y Cajal [94] in 1893, in the course of his seminal studies on Developmental Neuroscience. As recalled for instance in [105] and [27], Cajal noticed the remarkable behavior of growing axons of neurons, which maintain a precise orientation toward their target cells during their growth. As a matter of fact, for a mature nervous system to work properly, a very precise pattern of connections among a huge number of neurons (about 10^{12} in human brain) has to be established during embryonic and early postnatal periods, and such connections are made by migration of neurons from their proliferative sites to their eventual targets. Cajal considered what the mechanism could be for the "intelligent force" responsible for such guiding process. He eventually formulated in [94] the so-called neurotropic (or quimiotactic) theory, according to which target cells secrete attracting substances, and growing neuronal axons possess a chemotactic sensitivity (a "chemically induced ameboidism") that allow them to follow their way in the course of their motion toward their final destination (see Figure 1). In his later work on regeneration of the nervous system [96], Cajal observed that, in sectioned nerves, regenerating peripheral axons arising from proximal stumps will always go toward distal stumps, even if considerable obstacles are raised against their growth.

While these facts provided considerable support to the assumption of chemotactic guidance in neural navigation, the identification of the first molecules with chemotropic action in mammalian embryos took place a century afterward (cf. [104]). As a matter of fact, in a series of studies performed after 1980, a number of key features of neural wiring were ascertained, as for instance, the existence of intermediate targets that assist in keeping ax-

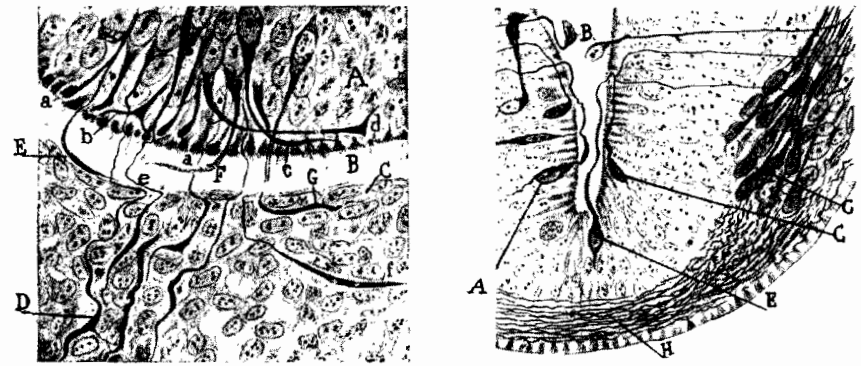

Fig. 1. Left: A section of early bone marrow (A) and mesodermic tissue taken from a three-day duck embryo. Notice that in younger neuroblasts growth cones always proceed in between the cells; E, F – growth cones freely moving through perimedular space; D – growth cones already placed at the mesodermal area. Right: Hystological preparation corresponding to the bulb of a four-days chicken embryo. Note that nervous fibers accidentally placed at the ventricule (A, E, C) appear to be free, and their axons orient themselves to move toward their destination through the nervous field. (Reproduced from [95].)

ons en route toward their final destinations [113], and the existence of repulsive molecules, that keep moving cells away from unwanted places [20]. In this way a scenario emerged in which neural navigation proceeds according to short-range cues and long-range, diffusive signals that may be either attractive or repulsive.

While neuroscience is arguably the field in which chemotaxis was first postulated, during the XX century a wealth of evidence has been accumulated, and considerable insight has been gained, on the role played by this type of directed motion in the life of a number of species.

One of these is the slime mold *Dictyostelium discoideum* (*Dd* for short), a kind of amoebae first identified by Raper in 1935 (cf. [97] and also [15]). These are nucleated cells that live in forest soils, feeding on bacteria. As long as there is sufficient food supply, *Dd* cells have a life cycle analogous to other microorganisms sharing the same habitat, and they proliferate by cell fission. However, when food becomes scarce, the social life of *Dd* amoebae is dramatically altered. To begin with, some cells start emitting pulses of a chemical (adenosine 3′,5′-cyclic monophosphate, cAMP) which acts as a communication signal. Cells are able to receive it, transduce it and then, after internally producing cAMP, they release it outside, thus keeping a cAMP feedback loop. As a consequence of this signaling process, amoebae eventually aggregate into mounds of rather constant size (up to 10^5 units), to form multicellular pseudoorganisms. These last subsequently enter into a developmental program which involves cell differentiation and migration, to eventually form a fruiting body which consists in a ball of spores (resistance forms that may remain in a quiescent state for several weeks) located on top of a thin stalk (for recent surveys, see [34,48,73], etc.). As observed for instance in [82], this clear separation in time from aggregation and differentiation makes *Dd* a suitable model organism to study in vivo both processes, that quite often occur simultaneously in other species.

Another biological model on which chemotaxis has been extensively studied is *Escherichia coli* (*E-coli*), a bacteria that usually colonizes the human bowel a few hours after birth, and which may be responsible for a number of serious infectious diseases. *E-coli* is able to swim toward sources of chemoattractants as aspartate or glucose by using as propellers the flagella it is provided with; see, for instance, [10] for a comprehensive description of *E-coli* behavior. White blood cells (and in particular neutrophils) provide a further example of chemotactic cells. For instance, neutrophils are known to navigate comparatively long distances to arrive at places in the body where injuries occur. An account of the physiological mechanisms which mediate chemotaxis in these (and others) types of cells can be found in [31], a monograph we refer to for additional information.

In spite of the considerable differences among such types of organisms (for instance, diameter lengths in *Dd* and *E-coli* differ by one order of magnitude), chemotactic cells present some common rules of functioning, governed by physical processes that may change from one species to other. To begin with, they should be endowed with a fine sensitivity, thus being able to detect small changes in chemoattractant concentrations around them. At the same type they should show adaptation, and therefore remain largely indifferent to important changes in homogeneous concentrations of otherwise stimulant chemicals. Once a (gradient) signal has been detected, they should be able to build up an amplified, internal signal transmission network strong enough to reorient its movement and yet sufficiently flexible to change direction again when necessary. Finally, in many instances

chemotactic migration involves coordinated motion of a large number of cells, which is regulated by intense intercellular communication.

In this chapter we shall review some of the quantitative models that have been proposed to account for some of the aforementioned aspects of chemotaxis. The term quantitative refers both to the physical assumptions, and the mathematical formulation thereof, which are advanced as a tool to gain insight in the way chemotaxis proceeds. As it will be apparent from our forthcoming discussion, quantitative modeling in chemotaxis is currently at a preliminary, although promising, level. Out of the various relevant features in chemotaxis, only a few will be addressed here, according to the plan which is briefly described below.

In Section 2 we shall be concerned with the actual manner in which individual chemotactic cells operate, and the limitations (and success stories) of such procedures will be described. In short, the line of thought goes as follows: cells detect changes in chemical gradients around them by monitoring the state of occupancy of specific receptors at their membranes, and they make use of the information thus gathered to trigger internal signaling cascades. Among other things, these last eventually result in cells oriented motion toward their targets. The discussion made in Section 2 deals therefore with individual cell behavior and their operating limits, and in this sense is not restricted to chemotactic cells, although the approaches to be described below have largely arisen in a chemotaxis setting.

Going from general to particular, in Section 3 we examine some of the mathematical problems whose study has been motivated by particular aspects of the cell cycle of *Dictyostelium discoideum*. As will be remarked then, some of these problems have become topics of mathematical interest in their own, so that their relation to the biological source has become fainter. In any case an attempt has been made to keep in mind the biological motivation as often as possible. A major issue to be addressed therein is pattern formation in *Dd* cultures. This is merely a part, however interesting, of a vast subject in which a huge literature is available. We have chosen to focus on a few topics, where mathematics has played a relevant role (and has benefited much from consideration of the problems involved). In few words, the questions examined in that section deal with early aggregation properties of *Dd* and the target-spiral transition which is customarily seen to mediate the establishment of aggregation centers.

In selecting such a reduced number of issues to address, many interesting features are left out; a particularly interesting example of this omission is cell motility. A second one (in a rather long list) concerns three-dimensional aspects of *Dd* culmination, of which only a few words will be said below. To such limitations in choice, restrictions in style will be added. Indeed, our approach will be basically descriptive, without going into the detail of mathematical proofs or arguments; for this we refer to the original sources where appropriate.

2. How do chemotactic units work?

To move toward a distant location, a cell should first receive a chemical cue released therein (or at some intermediate destination). This signal has then to be processed, to derive information about the position of the target it will eventually travel to. The first step in this process involves the interaction of signaling molecules (ligands) with specific receptors

located on the cell surface. These consist in macromolecules transversally inserted at the cell membrane. They thus possess an extracellular domain, where ligands land in, and an intracellular one. This last is instrumental in transducing signals by means of chemical processes (phosphorylation, methylation, ...) to trigger the subsequent cellular response.

It is natural to assume that a cell obtains information about, say, a source of chemoattractant from the state of occupancy of its membrane receptors (we say that a receptor is occupied as long as a ligand remains bound to it). To proceed in an efficient way, a cell should be able to monitor from that raw data the concentration of chemoattractant in its neighborhood. In particular, it has to detect small variations in its gradients (which may change their space distribution as time passes), a property often termed as sensitivity. Moreover, a fine sensitivity should go hand in hand with a high signal amplification downstream in the chemical cascade started by ligand binding to receptors. Amplification is required to set in motion the inner machinery of the cell, which will eventually result in navigation to a chemical target. Since cells move in media where chemical concentrations may vary over several orders of magnitude, it is necessary that the detection process be independent of the absolute concentration of isotropic ligands, a fact usually referred to as adaptation.

What does a cell know about the world around it? The physical limits to what a cell can actually measure were examined in a seminal article by Berg and Purcell in 1977 [11]. Some of the key points addressed in that work were succinctly described by the authors at their Introduction:

> "... In the world of a cell as small as a bacterium, transport of molecules is effected by diffusion, rather than bulk flow; movement is resisted by viscosity, not inertia; the energy of thermal fluctuation, kT, is large enough to perturb the cell's motion. In these circumstances, what are the physical limitations on the cell's ability to sense and respond to changes in its environment? What, for example, is the smallest change in concentration of a chemical attractant that a bacterium could be expected to measure reliably in a given time?"

In this section we shall review some of the mathematical approaches that have been proposed to gain insight into the key problem raised above: the manner in which a cell obtains information from receptor occupancy by ligand binding. To this end, we proceed in several steps. To start with, we shortly recall in the next subsection a basic model for ligand binding according to mass action law. This is done in an isotropic setting, and a formula for the equilibrium concentration is provided. We then discuss in Section 2.2 the role played by fluctuations in the distribution of receptor occupancy. In particular, it will be observed that, while ligand fluctuations are likely to be negligible, those in the kinetic binding process are rather important instead.

In Section 2.3 we consider the effect of diffusion (a particularly relevant type of mass transport) in the influx of ligands to a cell's surface. Of particular interest is the formula therein provided for the total current of ligands that may be absorbed by a system of N circular receptor patches scattered over the surface of a spherical cell (cf. (37), (38)). We then discuss in Section 2.4 the question of error measurement in two possible methods to measure ligand concentration from receptor occupancy: these are respectively known as spatial gradient and temporal gradient sensing. As a result, crude (but illuminating) estimates will be provided for the minimum gradient that can be detected, and the longest distance that a cell can navigate.

Impressive as these predictions are, cells are known to do even better. This they do by resorting to mechanisms only partially explored as yet. One of these is receptor clustering, which shall be dealt with in Section 2.5, where interaction of bivalent ligands with cell receptors is described in some detail, and analogies with polymerization processes are noticed. Understanding the precise manner in which clustering results in higher efficiency seems to require, however, of a detailed knowledge of the functioning of intracellular signaling pathways. This important topic will be dealt with in Section 2.6.

2.1. *Ligand binding to receptors*

In this and forthcoming subsections we shall borrow from a basic monograph due to Lauffenburger and Linderman [65], where fundamental aspects of receptor operation are described in detail. In its simplest setting, the process under consideration involves a monovalent ligand L that reversibly binds to a monovalent receptor R, to form a receptor–ligand complex C,

$$R + L \underset{k_r}{\overset{k_f}{\rightleftharpoons}} C, \tag{1}$$

where k_f (respectively k_r) denotes the kinetic rate of binding (respectively dissociation) of the process under consideration. According to the mass action law, a mathematical model for (1) is given by

$$\frac{dC}{dt} = k_f RL - k_r C. \tag{2}$$

To (2), some conservation laws should be added. In particular, the total number of receptors has to be preserved,

$$R + C = R_T, \tag{3}$$

and in many cases the amount of ligand may be assumed to remain unchanged during the process. If ligand concentration is measured in moles per volume, receptors are measured in number per cell and cells are present at concentration n (number per volume), one then has that

$$L + \frac{n}{N_A} C = L_0, \tag{4}$$

where $N_A = 6.02 \times 10^{23}$ is Avogadro's constant, giving the number of molecules per mole. If we further assume that $(n/N_A)C \ll L_0$, equations (2)–(4) simplify to

$$\frac{dC}{dt} = k_f (R_T - C) L_0 - k_r C, \tag{5}$$

that can be integrated to yield

$$C(t) = C_0 \exp\bigl(-(k_f L_0 + k_r)t\bigr) + \frac{k_f L_0 R_t}{k_f L_0 + k_r}\bigl(1 - \exp\bigl(-(k_f L_0 + k_r)t\bigr)\bigr). \tag{6}$$

Equation (6) describes rapid equilibration toward the steady-state value

$$C_{eq} = \frac{R_T L_0}{K_D + L_0} \quad \text{with } K_D = \frac{k_r}{k_f}, \tag{7}$$

where K_D is termed the equilibrium dissociation constant.

2.2. *The role of fluctuations*

In the previous deterministic model, the level of receptor occupancy is described by the formation of complexes C. However, a number of random factors may alter the values thus obtained. For example, random fluctuations in the ligand concentration near a cell may result in deviations from the values predicted by formulae (6) and (7). Following [65], we consider the effect of ligand random fluctuations on the equilibrium formula (7). The corresponding fluctuation in the number of complexes formed is given by

$$\delta C_{eq} = \frac{dC_{eq}}{dL}\,\delta L = \frac{R_T K_D}{(K_D + L)^2}\,\delta L, \tag{8}$$

where δC_{eq} denotes the standard deviation in C_{eq} as a result of a standard deviation δL in the value of L. The relative magnitude of these fluctuations in receptor binding is

$$\frac{\delta C_{eq}}{C_{eq}} = \left(1 + \frac{L}{K_D}\right)^{-1} \frac{\delta L}{L}. \tag{9}$$

To estimate $\delta C_{eq}/C_{eq}$ one thus needs an estimate for $\delta L/L$, and this last can be obtained from the formula

$$\frac{\delta L}{L} = (N_A L V)^{-1/2} \tag{10}$$

(cf. [11] and [65]). Here V is the volume of the medium accessible for ligand binding, and $N_A L V$ is the expected number of ligand molecules in that volume. A natural choice is $V \sim l^3$, where l is a characteristic length of the medium. For instance, if ligand transport is assumed to occur by a diffusion process with diffusivity D_L, then the distance traveled by an average molecule in a time t_* will be $l \sim (D_L t_*)^{1/2}$. If we take $t_* = k_r^{-1}$ (that is, the mean time period between receptor binding events), then at $L = K_D$ we would obtain

$$\frac{\delta L}{L} \sim \bigl(N_A (D_L k_r^{-1})^{3/2} K_D\bigr)^{-1/2}. \tag{11}$$

As pointed out in [65], for values $D_L \sim 10^{-6}$–10^{-5} cm^2/s, $k_r = 10^{-4}$–10^{-1} s^{-1}, $K_D = 10^{-10}$–10^{-6} moles/volume, (11) yields $\delta L/L \sim 10^{-7}$–10^{-2}, which by (9) translate into an estimate for $\delta C_{eq}/C \sim 10^{-5}$ to 1%.

Consider next the case of fluctuations in the kinetic binding process. In this context, rate constants may be given a probabilistic meaning. For instance, k_r can be thought of as the probability that a single complex will dissociate. Therefore, for $0 < \delta t \ll 1$, the probability of a single dissociation event at a given receptor will be $k_r\,\delta t$. More precisely, let $P_j(t)$ be the probability that there are j complexes on a cell at a time t. The change in the number of complexes occurring in a time interval δt, $0 < \delta t \ll 1$, assuming that there were C complexes at time t, is described by the kinetic equation

$$\begin{aligned} P_C(t+\delta t) - P_C(t) = {} & k_f L\bigl(R_T - (C-1)\bigr)P_{C-1}(t)\,\delta t \\ & - k_f L(R_T - C)P_C(t)\,\delta t \\ & - k_r C P_C(t)\,\delta t + k_r(C+1)P_{C+1}(t)\,\delta t. \end{aligned} \tag{12}$$

In the limit $\delta t \to 0$, this leads to

$$\begin{aligned} \frac{dP_C(t)}{dt} = {} & k_f L\bigl(R_T - (C-1)\bigr)P_{C-1} + k_r(C+1)P_{C+1} \\ & - \bigl(k_f L(R_T - C) + k_r C\bigr)P_C(t) \end{aligned} \tag{13}$$

for $C = 1, 2, \ldots, R_T - 1$. This set of equations is to be completed with

$$\frac{dP_0}{dt} = -k_f L R_T P_0 + k_R P_1, \tag{14}$$

$$\frac{dP_{R_T}}{dt} = k_f L P_{R_T - 1} - k_r R_T P_{R_T}. \tag{15}$$

Following a standard terminology, the set of equations (13)–(15) is customarily termed as the master equation for the process under consideration. To solve it, a classical method consists in introducing a generating function [38]

$$G(s,t) = \sum_{C=0}^{R_T} s^C P_C(t), \tag{16}$$

so that

$$P_0(t) = G(0,t), \qquad P_C(t) = \frac{1}{C!}\left[\frac{d^C G}{ds^C}\right]_{s=0} \quad \text{for } C = 1, \ldots, R_T - 1. \tag{17}$$

As a matter of fact, on multiplying each equation in (13)–(15) by s^C and then adding them up, one eventually obtains

$$\frac{\partial G}{\partial t} = (1-s)\left((k_f L s + k_r)\frac{\partial G}{\partial s} - k_f L R_T G\right). \tag{18}$$

To (18), the initial condition $P_C(0) = 0$ for $C \neq 0$, $P_C(0) = 1$ for $C = 0$ has to be added, which in terms of G reads

$$G(s,0) = 1. \tag{19}$$

Furthermore, the requirement that the sum of all probabilities be equal to one yields

$$G(1,t) = 1. \tag{20}$$

In many instances, we are interested in the mean value of C, denoted $\langle C \rangle$, and the variance σ_C^2. A quick check reveals that

$$\langle C \rangle = \sum_{C=0}^{R_T} C P_C = \left[\frac{\partial G}{\partial s}\right]_{s=1}, \tag{21}$$

$$\sigma_C^2 = \sum_{C=0}^{R_T} (C - \langle C \rangle)^2 P_C = \left[\frac{\partial^2 G}{\partial s^2} + \frac{\partial G}{\partial s} - \left(\frac{\partial G}{\partial s}\right)^2\right]_{s=1}. \tag{22}$$

Consider now the case of the steady-state solution of (18), obtained by setting $\partial G/\partial t = 0$ therein. We then may solve the resulting equation by direct integration, and then use (21), (22) to obtain

$$\langle C_{eq} \rangle = \frac{R_T L}{K_D + L}, \tag{23}$$

$$\delta C_{eq} \equiv (\sigma_C)_{eq} = \frac{(R_T L K_D)^{1/2}}{K_D + L}, \tag{24}$$

the last estimate being proportional to the total number of cell receptors R_T. From (23) and (24) it follows that

$$\frac{\delta C_{eq}}{C_{eq}} = \left(\frac{K_D}{L R_T}\right)^{1/2}.$$

In particular, when $L = K_D$ we obtain

$$\frac{\delta C_{eq}}{C_{eq}} = R_T^{-1/2}. \tag{25}$$

For instance, for $R_T = 10^4$ receptors/cell, statistical fluctuations with relative magnitude of 1% are expected, a value which falls well within the sensitivity threshold known for chemotactic cells [5,121]. On the other hand, a comparison of (25) with the corresponding value obtained at the end of our previous subsection reveals that this type of fluctuations is more likely to have an impact on chemotaxis then the previous one.

Concerning the time-dependent equation (18), we point out that the corresponding solution that satisfies (19) and (20) can be readily obtained by integration along characteristics (cf., for instance, [55]). Using then (21) and (22), it follows that

$$\langle C(t) \rangle = \frac{R_T L}{K_D + L}\left(1 - \exp\left(-(k_f L + k_r)t\right)\right), \tag{26}$$

$$\left(\sigma_C^2\right)_{eq} = \frac{R_T L}{(K_D + L)^2}\left(L \exp\left(-(k_f L + k_r)t\right) + K_D\right) \times \left(1 - \exp\left(-(k_f L + k_r)t\right)\right). \tag{27}$$

2.3. *Diffusion effects on ligand binding*

We have already noticed that diffusion has a limited influence on ligand fluctuations near the cells. However, this type of mass transfer process is the dominant mechanism to carry ligands toward the cells surface, so that reactions as that described in (1), (2) may occur. We shall briefly recall below some quantitative aspects of the role played by diffusion in the arrival of chemical signals at a cell.

To begin with, let us consider the following auxiliary problem. To determine the steady-state concentration of a ligand away from a single spherical cell, which is centered at the origin ($r = 0$) and whose surface corresponds to $r = R > 0$. One is thus led to solve

$$D\frac{1}{r^2}\frac{d}{dr}\left(r^2\frac{dL}{dr}\right) = 0 \quad \text{for } r > R. \tag{28}$$

Assuming constant concentration away from the cell, we require

$$L \to L_0 > 0 \quad \text{as } r \to \infty. \tag{29}$$

To solve (28), (29) an additional boundary condition has to be imposed at $r = R$. For later reference, we state below a choice of particular interest:

$$I \equiv 4\pi R^2 D\left[\frac{dL}{dr}\right]_{r=R} = k_{on} L(r) \quad \text{at } r = R,\ k_{on} \geqslant 0. \tag{30}$$

It is easy to check that the solution to (28)–(30) is provided by

$$L(r) = -\frac{k_{on} R L_0}{4\pi D R + k_{on}}\frac{1}{r} + L_0. \tag{31}$$

Suppose now that the whole surface of the cell is covered by receptors, and that ligands are instantly absorbed as soon as they arrive there. In this case, (30) has to be replaced by

$$L(r) = 0 \quad \text{at } r = R, \tag{32}$$

and the solution to (28), (29) and (32) is now given by

$$L(r) = L_0\left(1 - \frac{R}{r}\right) \quad \text{for } r > R, \tag{33}$$

so that the total flux carried out to $r = R$ is

$$I_M \equiv 4\pi R^2 D\left[\frac{dL}{dr}\right]_{r=R} = 4\pi R D L_0 \equiv k_+ L_0. \tag{34}$$

Relation (34) defines the observable association rate constant k_f. A second limit case of interest corresponds to the situation where there is only a single, circular receptor with radius s, $0 < s \ll R$, located over the cell surface ($r = R$), which is impervious to ligands except for the receptor patch. In this case (30) has to be replaced by

$$L = 0 \quad \text{at the receptor,} \qquad \frac{\partial L}{\partial r} = 0 \quad \text{otherwise over } r = R. \tag{35}$$

The solution to (28), (29) and (35), while still explicit, is not nearly as straightforward as that given by (31) or (33) (cf. [11] and [25], p. 42). The corresponding flux is now given by

$$4\pi R^2 D\left[\frac{\partial L}{\partial r}\right]_{r=R} = 4DsL_0. \tag{36}$$

Bearing in mind the two extreme cases (32) and (36), an asymptotic formula was derived in [11] corresponding to the case where the number of receptors N is large ($N \gg 1$), but the average distance d_s among them satisfies $d_s \gg s$, so that they are fairly separated from each other. A geometrical argument reveals that this is the case if $N^{1/2}s \ll R$. The estimate obtained in [11] reads

$$I = I_M \frac{Ns}{Ns + \pi R}. \tag{37}$$

Actually, a correction to formula (37) was later provided in [122] by means of an effective-medium argument, namely

$$I = I_M \frac{Ns}{Ns + \pi R(1 - p_A)}, \qquad p_A = \frac{N\pi s^2}{4\pi R^2}, \tag{38}$$

so that p_A represents the fraction of the sphere's surface which is covered with circular receptors. A striking consequence of (37) is that a large incoming flux can be achieved with relatively few, well-separated receptors. For instance, according to (37), $I = I_M/2$ if $N = \pi R/s$. If $R = 5$ μm (1 μm $= 10^{-6}$ meters) and $s = 10$ Å (1 Å $= 10^{-10}$ meters), the value $I_M/2$ is achieved when $N \sim 15.700$, the average distance among receptors is 1400 Å, and only a fraction of about 10^{-4} of the cell surface is covered by receptors [9].

Let us elaborate a bit on some of the formulae previously obtained. To this end, we follow [65] and observe that the binding of two molecules, as denoted by (1), is, in fact, a two-step process. First, molecular transport of the species R and L is required; we denote the corresponding rate constant by k_f. In our case, that transport is assumed to be due to diffusion. Then a chemical reaction takes place, which is characterized by the intrinsic association (respectively, dissociation) rate k_{on} (respectively, k_{off}). Thus the kinetic constants k_f, k_r in (1) are actually combinations of k_f, k_{on} and k_{off} described before. Moreover, constant D in (28) is such that $D = D_L + D_R$, the sum of ligand and receptor diffusivities. On the other hand, if a receptor is present at $r = R$, one has to write $k = k_{on}$ in (30). In this case, the forward rate k_f is given by

$$k_f = L_0^{-1} 4\pi R^2 D\left[\frac{dL}{dr}\right]_{r=R}. \tag{39}$$

Recalling the definition of k_{on}, k_+ in (30) and (34) respectively, one deduces from the previous remarks and (30) that

$$k_f = \frac{4\pi DRk_{on}}{4\pi DR + k_{on}} \equiv \frac{k_+ k_{on}}{k_+ + k_{on}} = \left(\frac{1}{k_+} + \frac{1}{k_{on}}\right)^{-1}. \tag{40}$$

As pointed out in [65], this formula allows for an appealing interpretation: the overall resistance to binding, denoted by $1/k_f$, is the sum of the resistance to diffusion $1/k_+$ and that to reaction $1/k_{on}$. In particular, if $k_{on} \gg k_+$, $k_f \sim k_+ = 4\pi DR$ and the binding is termed diffusion-limited. Conversely, when $k_{on} \ll k_+$, $k_f \sim k_{on}$ and the binding is considered to be reaction-limited.

2.4. *Estimating the measurement error*

In general, chemotactic cells move along paths for which their receptor occupancy gradient (spatial or temporal) is maximum. However, changes in occupancy are often so small that they hardly can be distinguished from fluctuations inherent to ligand binding. One many therefore wonder what are the physical limits imposed on a cell's ability to detect a chemical gradient.

To address this issue, we shall take up the analysis introduced in [11] and then developed in [28,29]. We shall roughly proceed as follows. One first assumes the incoming signal to be a function of the receptor occupancy. Then an estimate on the standard deviation about the mean signal is obtained, which is in turn used to derive a lower bound on gradient detection.

Consider first the case of a hypothetical mechanism based on spatial gradient detection. Such procedure requires estimating occupancy variations along a dimension parallel to the gradient. As before, we denote by L the ligand concentration around a cell, and write $p(L, t)$ to represent the associated fractional receptor occupancy. It is natural to assume that p arises as an average of a random variable describing ligand binding to receptors. If the cell is assumed to be spherical, and the concentration change across its diameter is given

by ΔL, the changes in ligand concentration and occupancy across a diameter will respectively be given by $(L+\Delta L)$ and $p(L+\Delta L,t)$. For a (nearly) constant gradient $\partial L/\partial x$, we have that

$$\Delta L \sim R\frac{\partial L}{\partial x}, \tag{41}$$

R being the cell's diameter. As a measure of the signal received, we may take

$$S=\frac{1}{T}\int_0^T \big(p(L+\Delta L,t)-p(L,t)\big)\,\mathrm{d}t, \tag{42}$$

where $T>0$ is an averaging time. The minimal requirement for a gradient to be detected is

$$S>\sigma, \tag{43}$$

where $\sigma(L,t)$ is the standard deviation in the measured occupancy, which is given by

$$\sigma^2(L,t)=\left\langle\left(\frac{1}{T}\int_0^T p(L,t)\,\mathrm{d}t\right)^2\right\rangle-\left\langle\frac{1}{T}\int_0^T p(L,t)\,\mathrm{d}t\right\rangle^2. \tag{44}$$

Estimating σ^2 in (44) involves dealing with the corresponding autocorrelation functions [11,28]. Arguing as in [28], one may show that

$$\sigma^2(L,t)=\frac{2}{NT^2}\int_0^T \mathrm{d}t\int_0^t p(s)\big(1-p(s)\big)\exp\left(-\int_s^t\frac{\mathrm{d}n}{\tau}\right)\mathrm{d}s,$$

where N is the number of receptors per cell, $p(s)$ is the fractional occupancy at time s and τ is the relaxation time for ligand–receptor binding (which also depends on time). From (41), and assuming $\Delta L \ll L$, one readily sees that

$$p(L+\Delta L)-p(L)\sim R\frac{\partial L}{\partial x}\frac{\partial p}{\partial L}, \tag{45}$$

whence

$$S\sim\frac{R}{T}\frac{\partial L}{\partial x}\int_0^T\frac{\partial p}{\partial L}\,\mathrm{d}t,$$

and condition (43) reads

$$\left(\frac{R}{T}\frac{\partial L}{\partial x}\int_0^T\frac{\partial p}{\partial L}\,\mathrm{d}t\right)^2>2\sigma^2(L,t) \tag{46}$$

(cf. [29]), where we have made use of the assumption $\sigma^2(L,t)\sim\sigma^2(L+\Delta L,t)$ for $\Delta L\ll L$.

A second detection mechanism is based in measuring temporal gradients. These arise as cells move through a spatial gradient. In this case, in order to measure the signal we consider the expression

$$S=\frac{1}{T}\int_{t_1}^{T+t_1}p(L+\Delta L,t)\,\mathrm{d}t-\frac{1}{T}\int_0^T p(L,t)\,\mathrm{d}t, \tag{47}$$

where $\Delta L\sim vt_1\partial L/\partial x$ and v denotes the cell velocity through the spatial gradient $\partial L/\partial x$. From (47) and (43) we thus obtain a condition for temporal gradient detection,

$$\frac{1}{T^2}\left(\int_{t_1}^{T+t_1}p(L,t)\,\mathrm{d}t+vt_1\frac{\partial L}{\partial x}\int_{t_1}^{T+t_1}p(L,t)\,\mathrm{d}t-\int_0^T p(L,t)\,\mathrm{d}t\right)^2 > \sigma^2(L,T+t_1)-\sigma(L,t). \tag{48}$$

Consider now the case of chemical equilibrium. Then there holds

$$p=\frac{KL}{1+KL},\quad \text{where } K=K_{\mathrm{D}}^{-1}=\frac{k_{\mathrm{f}}}{k_{\mathrm{r}}} \tag{49}$$

(see (7)), so that

$$\frac{\partial p}{\partial L}=\frac{K}{(1+KL)^2}, \tag{50}$$

and (44) yields now

$$\sigma^2(L,t)=\frac{2KL\tau}{NT(1+KL)^2},\qquad \frac{1}{\tau}=k_{\mathrm{f}}L+k_{\mathrm{r}} \tag{51}$$

(cf. (6) for the second statement above). Since $\tau/T\to 0$ at equilibrium, condition (46) gives

$$\frac{T}{\tau}>\frac{4(1+KL)^2}{KLN}\left(\frac{R}{L}\frac{\partial L}{\partial x}\right)^{-2}\equiv u_{\mathrm{s}}. \tag{52}$$

Note that u_{s} in (52) can be thought of as the minimum value of T/τ needed to detect a spatial gradient, under the assumption that equilibrium is rapidly arrived at.

For temporal gradient detection instead, and assuming that (49) holds, the first and third integrals in the left-hand side of (48) cancel out, and we obtain

$$S^2=\left(vt_1\frac{\partial L}{\partial x}\frac{\partial p}{\partial L}\right)^2=\left(\frac{kvt_1}{(1+KL)^2}\frac{\partial L}{\partial x}\right)^2=\left(\frac{Kt_1}{(1+KL)^2}\frac{\partial L}{\partial t}\right)^2. \tag{53}$$

Taking into account (51) and (53), we obtain the condition

$$\frac{T}{\tau}>\frac{4(1+KL)^2}{KLN}\left(\frac{t_1}{L}\frac{\partial L}{\partial t}\right)^{-2}\equiv\left(\frac{R}{vt_1}\right)u_{\mathrm{s}}, \tag{54}$$

where u_s is as in (52).

We are now ready to compare the relative efficiency of both detection mechanisms previously described. Consider first the case of spatial gradient detection, and assume that at chemical equilibrium n more receptors are occupied on the high concentration side of the cell that on the low concentration one. Then, from (45) and (50) it follows that

$$n = R\frac{\partial L}{\partial x}\frac{KN}{(1+KL)^2}.$$

From this and (52) one has

$$\bar{u}_s = \frac{4N}{n^2}\frac{KL}{(1+KL)^2}. \tag{55}$$

Since $f(x) = x(1+x)^{-2}$ has a maximum at $x = 1$, we readily see from (55) that $\bar{u}_s$ has a maximum at $KL = 1$. When the number of receptors N is of order $N \sim 10^4$–10^5, we thus obtain:

$$\frac{10^4}{n^2} \leqslant u_s \leqslant \frac{10^5}{n^2}. \tag{56}$$

As observed in [29], (56) sets a severe limitation on the possibility of detecting small occupancy differences. Suppose for instance that $n \sim 10$. Then $u_s \sim 10^2$–10^3, and according to (52) the averaging time T will be of the order of seconds if $\tau \sim 10^{-3}$ s, and in the range of hours to days if τ is of the order of seconds to minutes. When we particularize to bacterial cells as *E-coli*, the first situation is known to occur (that is, $\tau \sim 10^{-3}$ s) which in view of (51) requires dissociation constants of the order of 10^{-3} s^{-1}. Since a typical reaction-limited forward rate lies in the order of 10^5–10^6 s^{-1}, only low-affinity ligand binding would be allowed in this case.

Let us examine now the case of temporal gradient detection. Assuming again chemical equilibrium, one obtains from (49) and (47) that

$$S \sim \frac{K v t_1}{(1+KL)^2}\frac{\partial L}{\partial x}.$$

Recalling (51) and (48), signal and noise are now comparable when

$$T \sim 4\tau\left(\frac{R}{vt_1}\right)^2 \frac{KLN}{(1+KL)^2 n^2}. \tag{57}$$

Consider for instance the case where $KL = 1$, $N \sim 3 \times 10^3$. Then (57) yields $T \sim 3 \times 10^4 \tau (R/vt_{1n})^2$, which is to be compared with $T \sim 3 \times 10^4 \tau / n^2$ obtained in the case of spatial gradient sensing (see (54)). As pointed out in [29], this example shows that for $vt_1 \sim R$, temporal sensing offers no advantage over spatial sensing. A further point

to be noticed is that for a temporal sensing mechanism, the time T_0 required to detect a gradient is

$$T_0 \sim T + t_1,$$

which in view of (57) reads

$$T_0 \sim \frac{4\tau KLNR}{(1+KL)^2 v}\frac{1}{n^2 t_1^2} + t_1. \tag{58}$$

Since, for $B > 0$, $g(t_1) = B/t_1^2 + t_1$ achieves a minimum at $t_1 = (2B)^{1/3}$, (58) provides a way of estimating the minimum time to detect a gradient by a temporal mechanism. To that end, the key parameter turns out to be the ratio $(NR^2\tau/v^2n^2)$. As discussed in [29], the picture that emerges can be roughly described as follows. For small bacterial cells, the temporal mechanism permits detection of affinities 10^2–10^3 higher that could be obtained from a spatial mechanism (see Figure 3 in [29]). However, for large crawling cells the affinity range on which temporal detection fares better is much more restricted, and spatial detection becomes more efficient for low affinity ligands (Figure 4 in [29]).

What is the maximum distance that a cell can navigate in the trail of a chemical scent? A simple estimate can be provided by requiring that the ligand should have a relative concentration change across the cell diameter which is equal to the minimum required for gradient detection [40]. Recalling (10), we thus obtain

$$\frac{R}{L}\frac{\mathrm{d}L}{\mathrm{d}x} = (N_A L V)^{-1/2}.$$

In fact, arguing as in [11], the right-hand side in the equation above can be replaced by a more precise estimate, namely,

$$\frac{R}{L}\frac{\mathrm{d}L}{\mathrm{d}x} = \left(2\pi T D R\left(\frac{N_s}{N_s + \pi a}\right)\left(\frac{K_D L}{K_D + L}\right)\right)^{-1/2}, \tag{59}$$

where D is the ligand diffusion coefficient and T is the total averaging time (cf., for instance, (46)). Solving for $\mathrm{d}x$ gives

$$\mathrm{d}x = R\left(2\pi T D R\left(\frac{N_s}{N_s + \pi a}\right)\left(\frac{K_D L}{K_D + L}\right)\right)^{1/2}\frac{\mathrm{d}L}{L}. \tag{60}$$

Equation (60) has to be supplemented with suitable initial values. A proposal made in [40] is that

$$L = L_{\max} \quad \text{at } x = 0. \tag{61}$$

The maximum guidance distance $x = x_M$ is then defined by

$$L = 0 \quad \text{at } x = x_M. \tag{62}$$

Assuming $L_{\max} \sim 100K_D \gg K_D$, an analysis in [40] yields

$$x_M \sim 1 \text{ cm}, \tag{63}$$

which seems to be a good estimate for the case of neural navigation. Notice that, when rescaled in an appropriate way, (63) corresponds to a distance of $\sim$1 km for an organism of the size of a human being.

2.5. *Receptor clustering*

While the performance predicted by the models described before is fairly good, it has become apparent that cells can do even better. For that reason, the assumptions initially made in [11] were thoroughly revised later, in an attempt to match the experimental facts observed. This led to extensive work on two issues to be considered in our forthcoming sections: the control properties of the intracellular signaling cascade, and the cooperative effects derived from receptor clustering. We shall leave the first from these for the following section, and will concentrate in the second one herein.

It was long since noticed that the nature of the cell membrane allows for lateral mobility of receptors; actually, an estimate on receptors diffusivity was derived as early as in 1975, see [100]. On the other hand, the relevance of multiple attachment to multifunctional ligands (only the monovalent case was considered in [11]) was soon recognized. As it is often the case, theoretical analysis came first (cf. [89–91]) and structural information on the nature of the process was available later (see, for instance, [58,71]).

We shall next describe the early model for receptor clustering proposed by Perelson and De Lisi on [91]. These authors considered the case of reversible binding of bivalent ligands under the assumption (subsequently weakened) that ligands are endowed with two functional units, that may bind to different receptors.

Following [91], let us denote by $L(t)$ the concentration of free ligand in the medium at time t. Suppose that at $t = 0$ all ligand is unbound, and write $L(0) = L_0$, but for later times it can reversibly bind to a receptor with forward (respectively reverse) kinetic constant k_1 (respectively k_{-1}). Let S_0 be the total concentration of receptor sites, present in number n, so that $S_0 = n\overline{S_0}$ where $\overline{S_0}$ is the receptor concentration. Write also $S(t)$ to represent the concentration of free receptor sites at time t. Finally, let $m(t)$ and $M(t)$ respectively denote the concentrations of singly and doubly bound ligands. In order to cross-link two receptors, a free functional group can bind a receptor site located nearby with a rate constant k_2. If we denote by k_{-2} the kinetic constant for dissociation of a functional group in a doubly bound ligand, one readily arrives at the following system:

$$\frac{dm}{dt} = k_1 LS - k_{-1}m - k_2 mS + 2k_{-2}M, \tag{64}$$

$$\frac{dM}{dt} = k_2 mS - 2k_{-2}M, \tag{65}$$

with initial conditions $m(0) = M(0) = 0$. On the other hand, conservation of ligand and conservation of receptor sites yield the relations

$$L_0 = L(t) + m(t) + M(t), \qquad S_0 = S(t) + m(t) + 2M(t). \tag{66}$$

Notice that the model describes the state of the system consisting of cellular receptors and ligand molecules by means of the state of the ligand (free, singly or doubly bound) only. Moreover, knowing that a ligand is singly or doubly bound, does not permit to derive information about the aggregate it is attached to. Furthermore, an equivalent-site hypothesis is also done: no distinction is made between free receptor sites on aggregates of different length, nor between free ligand sites. Finally, intramolecular rearrangements leading to rings of n crossed-linked receptors are also discarded at this stage (although a suitable modification of the model can accommodate such assumption; cf. Section IV in [91]; see also [93]). After discussing the nature of equilibrium solutions to (63)–(65), the question of the distribution of ligand–receptor aggregates in the cell surface is also addressed in [91]. Consider for instance the case of linear chains formed by the interaction of bivalent ligands and bivalent receptors, so that singly bound ligands can only occur at the ends of a chain. Let $c_j(n,t)$ be the concentration of aggregates containing j, $j = 0, 1, 2$, singly bound ligands and n receptors. Then, for $n = 1, 2, 3, \ldots$,

$$\begin{aligned}\frac{dc_0(n)}{dt} &= -2k_1 Lc_0(n) + k_{-1}c_1(n) \\ &\quad - 2k_2 c_0(n)\left(\sum_{i=1}^{\infty} c_i(i) + 2\sum_{i=1}^{\infty} c_2(i)\right) \\ &\quad + 2k_2 \sum_{i=1}^{n-1} c_0(i)c_i(n-i) - 2(n-1)k_{-2}c_0(n) \\ &\quad + k_{-2}\left(2\sum_{i=n+1}^{\infty} c_0(i) + \sum_{i=n+1}^{\infty} c_1(i)\right),\end{aligned} \tag{67}$$

$$\begin{aligned}\frac{dc_1(n)}{dt} &= 2k_1 Lc_0(n) - k_1 Lc_1(n) - k_1 c_1(n) + 2k_{-1}c_2(n) \\ &\quad - k_2 c_1(n)\left(2\sum_{i=1}^{\infty} c_0(i) + 2\sum_{i=1}^{\infty} c_1(i) + 2\sum_{i=1}^{\infty} c_2(i)\right) \\ &\quad + 4k_2 \sum_{i=1}^{n-1} c_0(i)c_2(n-i) + k_2 \sum_{i=1}^{n-1} c_1(i)c_1(n-i) \\ &\quad - 2k_{-2}(n-1)c_1(n) + 2k_{-2}\sum_{i=n+1}^{\infty}\left(c_0(i) + c_1(i) + c_2(i)\right)\end{aligned} \tag{68}$$

and

$$\frac{dc_2(n)}{dt} = k_1 L c_1(n) - 2k_1 c_2(n) - 2k_2 c_2(n) + \left(\sum_{i=1}^{\infty} c_1(i) + 2\sum_{i=1}^{\infty} c_0(i)\right)$$
$$+ 2k_2 \sum_{i=1}^{n-1} c_1(i)c_2(n-i) - 2(n-1)k_{-2}c_2(n)$$
$$+ k_{-2} \sum_{i=n+1}^{\infty} \big(c_1(i) + 2c_2(i)\big). \tag{69}$$

Equations (66)–(68) make up an infinite system of coupled nonlinear differential equations which is reminiscent of Smoluchoswski's system for the coagulation of colloids (cf., for instance, [19]). This last has been widely used to model polymerization and aerosol dynamics (see [36]), and in a simple setting can be formulated as follows. Let $c_n(t)$ denote the concentration at time t of chains consisting of n ($n \geqslant 1$) identically functional monomers. Assuming monomer aggregation to be irreversible, the c_n's satisfy

$$\frac{dc_n}{dt} = \frac{1}{2} \sum_{i+j=n} a_{ij} c_i c_j - c_n \sum_{j=1}^{\infty} a_{nj} c_j, \tag{70}$$

where $\{a_{nj}\}$ represent the coagulation coefficients of the process under consideration. If we take all a_{nj} to be equal to a positive constant (Smoluchowski's original assumption), the close relation between (70) on one hand, and (67)–(69) becomes apparent. Actually, for monodisperse initial values (that is, for $c_1(0) = c_0 > 0$ and $c_n(0) = 0$ for $n \geqslant 2$), system (70) with constant coefficients can be explicitly solved ([19,36]), and the same happens for (67)–(69). More precisely, if we take

$$c_0(1,0) = \frac{S_0}{2},$$
$$c_0(n,0) = 0 \qquad \text{for } n > 1,$$
$$c_1(n,0) = c_2(n,0) = 0 \quad \text{for } n \geqslant 1,$$

then a combinatorial argument described in [91] reduces the solution of (67)–(69) to that of (64)–(66). More precisely, there holds

$$c_j(n,t) = \frac{S_0}{2}\binom{2}{j}\left(\frac{m}{S_0}\right)^j \left(\frac{2M}{S_0}\right)^{n-1} \left(\frac{S}{S_0}\right)^{2-j}, \quad j = 0,1,2. \tag{71}$$

To keep this chapter within reasonable bounds, we shall refrain from discussing the cases of aggregates with rings (for which we refer to Section IV in [91]), ligands with chemically distinct functional groups (considered in [89]), or multivalent ligands, which is analyzed in [90].

At this juncture, the question arises of ascertaining the comparative performances of receptor clustering vs systems of scattered receptors. Actually, we have already noticed that, under the assumptions on receptor nature made in [11], a cluster of receptors would result in a lower efficiency with respect to that of a similar number of well-separated receptor units. The mechanisms by which clustering provides an evolutionary advantage remain largely to be elucidated. Recent research points to amplification in the downstream signaling cascade as (at least part of) an explanation. We shall return to this point in our next section, where properties of intracellular chemical pathways will be considered. We just quote on pass that it has been recently suggested that oligomer formation could actually buffer intracellular signaling against stochastic fluctuations (cf. [1]). In the same work it is also proposed that long linear oligomers increase the range of ligand concentration to which the cell may respond, whereas long closed oligomers seem to favor ligand specificity; see also [2] for related material.

2.6. *Signaling pathways and their performance properties*

In previous subsection, we have been concerned with the physical mechanisms by which a cell derives information from the concentration of ligands near its surface. We now discuss the properties of signaling pathways. In particular, their ability to amplify signals received as well as to adapt to homogeneous (but largely fluctuating) external ligand concentration will be examined.

It has been already mentioned that chemotactic cells possess a fine sensitivity, that allows them to detect ligand gradients of 1–2% across their surface [5,121]. It is known that these minute differences are internally amplified (even by a factor ~55, cf. [103]). The question naturally arises of understanding the structure of the chemical circuits involved and the output they can provide. To address this issue, we shall begin by following Heinrich, Neel and Rapoport [45] to examine the properties of some simple, although relevant, types of signaling pathways. To that end, let us consider a linear signaling cascade in which stimulation of a receptor leads to consecutive activation of several protein kinases. The eventual output is the phosphorylation of the last kinase, which usually triggers a cellular response (as for instance, activation of a transcription factor). Signaling is inhibited by phosphatases (which dephosphorylate the kinases), and by inactivation of the receptor. To proceed, suppose that each phosphorylation step is described as a reaction between the phosphorylated form X_{i-1} and the nonphosphorylated form $\widetilde{X}_i$ of the ith kinase. Assume that the phosphorylation rate is given by $\nu_{p,i} = \tilde{\alpha}_i X_{i-1}\widetilde{X}_i$, and the dephosphorylation rate by $\nu_{d,i} = \beta_i X_i$, for some kinetic parameters $\tilde{\alpha}_i$, β_i. Then the overall process can be represented as follows:

$$\frac{dX_i}{dt} = \nu_{p,i} - \nu_{d,i} = \tilde{\alpha}_i X_{i-1}\widetilde{X}_i - \beta_i X_i \quad \text{for } 2 \leqslant i \leqslant n,$$

where n denotes the total number of subsequently activated kinases, and

$$\frac{dX_1}{dt} = \tilde{\alpha}_i R(t)\widetilde{X}_1 - \beta_1 X_1.$$

Here $R(t)$ is the concentration of activated receptors as a function of time. If we now denote by $C_i = X_i + \widetilde{X}_i$, $i \geqslant 1$, the total amount of kinase i, and set $\alpha_i = \tilde{\alpha}_i C_i$, the equations above read

$$\frac{dX_1}{dt} = \alpha_1 R(t)\left(1 - \frac{X_1}{C_1}\right) - \beta_1 X_1, \tag{72}$$

$$\frac{dX_i}{dt} = \alpha_i X_{i-1}\left(1 - \frac{X_i}{C_i}\right) - \beta_i X_i, \quad 2 \leqslant i \leqslant n. \tag{73}$$

To (72), (73) we now add initial values given by

$$X_i(0) = 0, \quad 1 \leqslant i \leqslant n, \qquad R(0) = R > 0. \tag{74}$$

Moreover, we assume for simplicity that

$$R(t) = Re^{-\lambda t} \quad \text{for some } \lambda > 0. \tag{75}$$

Consideration of any signaling system (and, in particular, the previous one) leads to a number of natural questions. For instance, (i) How fast does the signal reaches its destination? (ii) How long does the signal lasts? and (iii) How can one measure the signal strength? To answer them, the authors of [45] introduce three parameters: the signaling time of the ith kinase, τ_i, given by

$$\tau_i = \frac{T_i}{I_i}, \quad 1 \leqslant i \leqslant n, \quad \text{with } I_i = \int_0^\infty X_i(t)\,dt, T_i = \int_0^\infty t X_i(t)\,dt, \tag{76}$$

provided that these integrals converge. Notice that τ_i is analogous to the mean value of a statistical distribution. For $1 \leqslant i \leqslant n$, the signal duration θ_i is defined as follows:

$$\theta_i^2 = \frac{Q_i}{I_i} - \tau_i^2, \quad \text{where } Q_i = \int_0^\infty t^2 X_i(t)\,dt, \tag{77}$$

once again, the integral above is assumed to converge, in which case θ_i is similar to the standard deviation of a statistical distribution. Finally, the signal amplitude S_i is defined through the relation

$$S_i = \frac{I_i}{2\theta_i}, \tag{78}$$

so that S_i is the height of a rectangle whose length is $2\theta_i$, and whose area is the same as that enclosed under the curve $X_i(t)$.

Let us briefly recall some of the consequences of the analysis performed in [45]. Consider first the case of weakly activated pathways, for which $X_i \ll C_i$ for any i. Then (73) reduces to

$$\frac{dX_i}{dt} = \alpha_i X_{i-1} - \beta_i X_i, \quad i \geqslant 2,$$

and the previous parameters can be explicitly computed. More precisely, let τ, θ, S be defined by

$$\tau = \sum_{i=1}^n \tau_i, \qquad \theta = \sum_{i=1}^n \theta_i, \qquad S = \sum_{i=1}^n S_i.$$

Then there holds

$$\tau = \frac{1}{\lambda} + \sum_{i=1}^n \frac{1}{\beta_i},$$

$$\theta^2 = \frac{1}{\lambda^2} + \sum_{i=1}^n \frac{1}{\beta_i^2}, \tag{79}$$

$$S = \frac{R}{2}\prod_{i=1}^n \frac{\nu_i}{\beta_i}\left(1 + \lambda^2 \sum_{i=1}^n \frac{1}{\beta_i^2}\right)^{-1/2}.$$

Note that τ, the signaling time through the whole pathway, and θ, the total signal duration, are independent of the kinase rate constants (in other words, they do not depend on the α_i's). However, the total signal amplitude does depend on all parameters involved in the system.

We say that amplification occurs at the ith step in the cascade if

$$\sigma_i = \frac{S_i}{S_{i-1}} > 1. \tag{80}$$

In the case under consideration, it follows from (79) that (80) is satisfied if

$$\beta_i < \alpha_i\left(1 - \frac{1}{\alpha_i^2 \theta_{i-1}^2}\right)^{1/2}, \tag{81}$$

provided that the quantity within braces is positive. As a matter of fact, it follows from (79) and (81) that longer pathways favor an increase in signaling time, signal duration and amplification in later stages of the signaling cascade.

When weak activation is no longer assumed, one has to deal with the whole system (72), (73). Assuming rapid equilibration; that is, setting $dX_i/dt = 0$ in (73), one obtains

$$X_i = C_i X_{i-1}\left(\frac{\beta_i}{\nu_i} C_i + X_{i-1}\right)^{-1}. \tag{82}$$

From (80) and (82), one readily sees that amplification occurs if

$$X_{i-1} < C_i\left(1 - \frac{\beta_i}{\nu_i}\right). \tag{83}$$

A comparison of (81) and (83) shows that signal amplification is less pronounced in this situation. Also an analysis of the case of a permanently activated pathway ($\lambda = 0$ in (75)) for a particular choice of C_i, α_i, β_i shows that amplification only occurs in this example if the activated receptor does not go beyond a threshold value, so that one needs $R < R_*$ for some $R_* > 0$; see Figure 5 in [45] for further details.

A situation also considered in [45] is crosstalk between signaling networks that are simultaneously operating. As an example, consider the case in which a component Y of a second pathway inhibits phosphatase i in the first scheme by changing its kinetic rate. This may be achieved, for instance, by replacing β_i in (73) by

$$\beta_i = \beta_i^0 \left(1 + \frac{Y}{K_i}\right)^{-1},$$

for some positive constants β_i^0, K_i. It is shown in [45] that crosstalk may have a considerable influence in the case of strong activation, and that it may provide amplification combined with fast and transient signaling.

A final point to be mentioned in this context is that of the stability of signaling networks. In many situations, it is required that random kinase fluctuations should be damped out. However, positive feedback loops are a possible source of instability. Indeed, if we replace (72) by

$$\frac{dX_1}{dt} = (\alpha_1 R + \varepsilon X_n)\left(1 - \frac{X_1}{C_1}\right) - \beta_1 X_1, \tag{84}$$

then instability of the ground state $R = X_i = 0$, $1 \leqslant i \leqslant n$, is obtained provided that

$$\beta_1 \beta_2 \cdots \beta_n < \varepsilon \alpha_2 \cdots \alpha_n. \tag{85}$$

On the other hand, from the last formula in (79) it follows that when $\lambda = 0$, the amplification condition at any step in the corresponding circuit reads

$$\beta_1 \beta_2 \cdots \beta_n < \alpha_1 \alpha_2 \cdots \alpha_n. \tag{86}$$

It turns out that sustained amplification can have a destabilizing effect in the presence of feedback loops. We refer to the reader to [45] for further discussion on this and other related topics.

The previous remarks were of a general nature. A different (but complementary) approach consists in analyzing particular situations where amplification is known to occur, in order to unravel the mechanisms that yield such result. A case which has deserved considerable attention is that of the phosphorelay sequence triggered in *E-coli* by the aspartate receptor *Tar*, which eventually connects with the flagellar motors through a pathway involving the *CheA*, *CheY* and *CheZ* proteins [3,58,106]. In particular, in [3] the authors addressed the issue of understanding the reasons for the high gain in the system. This was defined as the change of rotational bias divided by the change in receptor occupancy, and is estimated to be ~55 [103].

Out of the several reasons suggested to account for this outstanding performance, the authors of [3] hinted at the indirect activation of many receptors by a single ligand. Receptor clustering, which has been shortly discussed in our previous subsection, has been proposed as a model to enhance sensitivity. However, it has been observed that such mechanism, while seemingly improving sensitivity at low-concentration signals, presents considerable difficulties to simultaneously provide high gain and a wide dynamic range (see [17]).

The model discussed in [3] considers teams of *Tar* receptors (which are of a dimeric nature, cf. [58]) that assemble and disassemble to form teams of one, two or three units. It is assumed that ligand binding destabilizes receptor teams, which subsequently break into smaller units (ligands are not released in that process). A key hypothesis is that only ligand-free threefolds determine kinase activity. The authors remark that their model is able to explain the observed behavior of the kinase activity for a pure receptor under a number of assumptions that, in some cases, could be experimentally tested.

We next turn our attention to adaptation. In engineering terms, any given circuit (possibly representing a chemotactic cell), that can be characterized as producing an output signal ϕ in response to an input signal S is said to possess this property if the output ϕ remains constant when isotropic stimulation S is increased over several orders of magnitude. Bearing chemotaxis always in mind, a question that naturally arises is that of determining (relatively) simple circuits (modules), described by systems of chemical reactions, that display adaptation. Such modules are also expected to be robust. This means that their performance is not significantly altered when parameters in the model undergo large variations (up to some orders of magnitude).

A common feature in many of the models so far derived to account for adaptation is that they make use of activator–inhibitor systems. These last reflect the fact that many examples of biological pattern formation show the interplay of a local, self-enhancing reaction coupled to a long-range antagonistic reaction [39,76]. A typical example is provided by

$$\frac{\partial a}{\partial t} = \frac{\alpha a^2}{h} - \mu a + D_a \frac{\partial^2 a}{\partial x^2}, \tag{87}$$

$$\frac{\partial h}{\partial t} = \delta a^2 - \nu h + D_h \frac{\partial^2 h}{\partial x^2}, \tag{88}$$

where α, μ, δ and ν are kinetic constants, and D_a, D_h denote the respective diffusivities of substances a (activator) and h (inhibitor). Suppose for simplicity that constants α, μ, δ and ν are set equal to one, and assume that activator and inhibitor concentrations are constant in space, so that diffusion effects can be discarded. Then $a = h = 1$ is a solution of the associated kinetic system

$$\begin{aligned} \dot{a} &= \frac{a^2}{h} - a, \\ \dot{h} &= a^2 - h. \end{aligned} \tag{89}$$

According to these equations, if h remains constant and equal to one, and a becomes slightly larger than one, $\dot{a} > 0$ and a will increase further. Actually, should $h = 1$ continue

to hold, the first equation above would then yield finite-time blow-up for $a(t)$. Assume however that there is very rapid equilibration of the inhibitor to a given activator concentration. At the steady state ($\dot{h} = 0$) this gives $h = a^2$, which upon substitution in (89) yields in turn

$$\dot{a} = 1 - a,$$

whence $\dot{a} < 0$ for $a > 1$. In this way, stability of the equilibrium $a = 1$ is achieved. When space inhomogeneities are taken into account, so that a diffusion mass transport sets in, the rapid equilibration of h with respect to a can be achieved by taking $D_h \gg D_a$ in (87), (88), a condition whose relevance in pattern formation was already noticed in Turing's seminal work [114]. In this manner, nonlinear patterns emerge and become stable in (87), (88); see for instance [76] for a detailed discussion on this issue.

As noticed by Meinhardt in [77], this type of model is very convenient to detect minor external concentration differences and convert them into a pronounced intracellular pattern, even when the external signal is subject to random fluctuations. Amplification is thus obtained, and also adaptation, since this effect is rather independent of the value of an external, isotropic stimulus; see Figure 2.

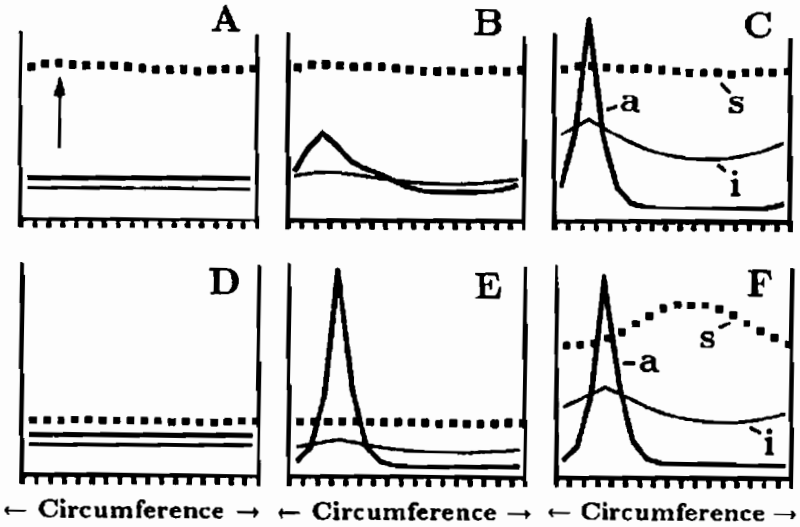

Fig. 2. Detection of minute asymmetries and the problem of reorientation. Assumed is a cell-internal pattern forming reaction consisting of a self-enhancing activator (a) and a long-ranging inhibitor (i). Sufficient for the localization of a strong internal signal is a noisy, slightly asymmetric external signal (s, black squares) that has a stimulating influence on the activator production. Simulations made on the circumference of a circle: the left and right elements are neighbors in reality. Shown is the initial (A), an intermediate (B) and the final stable distribution (C). A strong internal activator maximum appears at the position where the external signal is slightly above average (arrow in A). D, E – As required for path-finding in a graded environment, orientation works also at a much lower absolute level of the external signal. The lower signal concentration is compensated by a lower inhibitor concentration. F – The problem: after an incipient pattern has been formed, even a strong external asymmetry is unable to reorient the pattern. (Reprinted from [77], with permission granted by the Company of Biologists Ltd.)

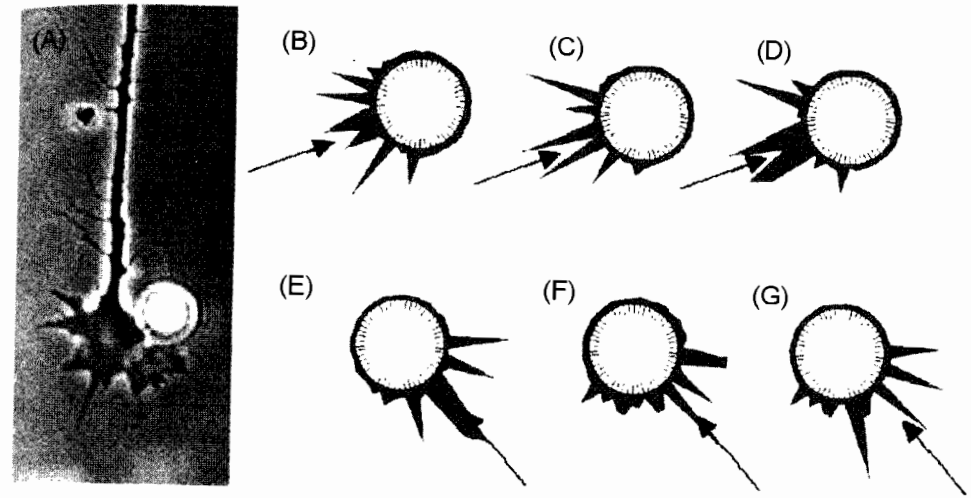

Fig. 3. Orientation of growth cones and chemotactic cells. A – A growth cone of a nerve growing in vitro. B, G – Model. Assumed is an internal pattern-forming system in which the self-enhancing process saturates and in which the activator does not diffuse; shown is only the activation. The distance from the inner circle is a measure for the local activation. The external orienting signal has a positive influence on the internal patterning system of the cell. The concentration difference across the cell is 2%; its orientation is indicated by the arrow. Assumed are max. 1% statistical variations in the cell cortex in the ability to perform the self-activation. B, D – Simulation: somewhat irregular active spots emerge that act as signals to stretch out cell extensions toward the signaling source. Due to their limited half-life caused by a local antagonistic process, they disappear subsequently and new ones emerge instead. E, G – After a change in the orientation of the external signal (arrow), the locations of the temporary signals adapt rapidly to the new direction. Thus, the system is able to detect permanently minute concentration differences (photograph kindly supplied by J. Loschinger). (Reprinted from [78], with permission from Elsevier.)

However, once the intracellular signal (the pattern) is formed, self-stabilization of that pattern is so strong that small external cues (as those actually at work in chemotactic processes) are unlikely to result in a reorientation. To deal with this difficulty, a mechanism was proposed in [77] that consists in including a second antagonistic reaction, to obtain an oscillating activator–inhibitor system. In this way, the cell (nerve growth cones are the example being considered in [77]) proceeds in a cyclic manner from phases where it is highly sensitive to external signals, to periods where weak external inputs are converted into strong internal patterns, that can be used to reorient the cell toward its target. This model is sketched in Figure 3, which is taken from [78].

A particular model where this behavior can be observed is

$$\begin{aligned} \frac{\mathrm{d}a}{\mathrm{d}t} &= \frac{\theta(a^2 b^{-1} + \alpha)}{(\beta + c)(1 + \delta a^2)} - \mu a, \\ \frac{\mathrm{d}b}{\mathrm{d}t} &= \nu(a - b), \\ \frac{\mathrm{d}c}{\mathrm{d}t} &= \omega a - \tau c, \end{aligned} \tag{90}$$

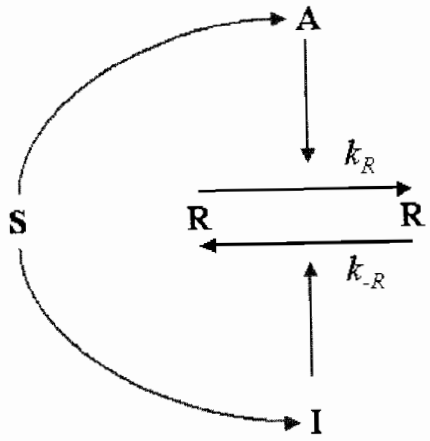

Fig. 4. A schematic representation of system (91)–(93) (adapted from [70]).

for suitable choices of the parameters δ, α, β, δ, μ, ν, ω and τ therein (see the Appendix in [77]). Actually, in (90) the external signal (and its changing orientation) is lumped in parameter θ, where random fluctuations are also incorporated.

We next discuss a conceptually simple scheme for perfect adaptation to spatially uniform changes in ligand concentration that has been proposed in [70] (see also [62,53]). Its ingredients are as follows. For any given species Z, let us denote by Z_T its total concentration, and by Z^* that of its active form. Suppose that a response element R may go from an active to an inactive state, and that passage from R to R^* (respectively, from R^* to R) is mediated by an activator A (respectively, by an inhibitor I), both of which are produced from an external signal S. We may graphically represent this circuit in Figure 4.

In mathematical terms, the previous scheme can be written in the form

$$\frac{dR^*}{dt} = -k_{-R} I R^* + k_R A\big(R_T - R^*\big), \tag{91}$$

$$\frac{dA}{dt} = -k_{-A} A + k'_A S(A_T - A), \tag{92}$$

$$\frac{dI}{dt} = -k_{-I} I + k'_I S(I_T - I). \tag{93}$$

To make the analysis simpler, let us assume that $A_T \gg A$, $I_T \gg I$. Then (91)–(93) reduces to

$$\frac{dR^*}{dt} = -k_{-R} I R^* + k_R A R, \tag{94}$$

$$\frac{dA}{dt} = -k_{-A} A + k_A S, \tag{95}$$

$$\frac{dI}{dt} = -k_{-I} I + k_I S, \tag{96}$$

where $k_a = k'_a A_T$, $k_I = k'_I I_T$, and the various remaining constants in (91)–(93) are kinetic parameters of the process under consideration. At the steady state, we should have

$$\overline{R^*} = \left(\frac{\overline{A}/\overline{I}}{k_D + \overline{A}/\overline{I}}\right) R_T, \tag{97}$$

where $\overline{Z} = \lim_{t\to\infty} Z(t)$ for any given variable Z, and $k_D = k_{-R}/k_R$ as in (7). Note that (95)–(96) yield, at the steady state

$$\overline{I} = k_1 \overline{S}, \quad k_1 = \frac{k_I}{k_{-I}}, \qquad \overline{A} = k_2 \overline{S}, \quad k_2 = \frac{k_A}{k_{-A}},$$

and therefore (97) corresponds to perfect adaptation: the value of $\overline{R^*}$ provided in that formula remains unchanged when $S(t)$ is replaced by $\alpha S(t)$ for any $\alpha > 0$.

The kinetic system (94)–(96) has some drawbacks when considered as a building block for a model that should provide spatial sensing with high gain. For instance, suppose that an external source varies linearly along the length of the cell, so that $S(x) = c_0 + c_1 x$ for some constants c_0, c_1, where x is a normalized distance measured, say, along a cell diameter. Assume for simplicity that the activator A does not diffuse but the inhibitor I does so according to the equation

$$\frac{\partial I}{\partial t} = -k_{-1} I + k_I S + D\Delta I,$$

which should replace (96) in system (94)–(96). An analysis as that described in [62] shows that

$$\overline{R^*}(x) \sim \frac{1}{1 + f(x)} \quad \text{for some } f(x) \geqslant 0,$$

so that this model does not provide gain in the difference of activity between the front and the rear of the cell with respect of that of the external signal. A way to remedy this situation consists in increasing the complexity of the kinetic scheme under consideration. This may be achieved, for instance, by replacing the process depicted in Figure 4 by that in Figure 5.

The onset of asymmetry in a chemotactic cell after a rise in external signal is often the first noticeable step in the subsequent directional sensing process. This issue has been addressed in [98] in the context of studies conducted on the slime mold *Dictyostelium discoideum* (*Dd*). The situation succinctly described in [98] is as follows. An applied cAMP signal, way larger than that required to trigger a response, is applied to a medium with *Dd* cells. This signal will quickly diffuse around any individual cell, from front to back. Since cAMP receptors are thought to be uniformly distributed over the cell's membrane, it is natural to assume that an inhibitory mechanism should appear that suppresses responses at the cell's back (measured with respect to the cAMP source introduced). Once an initial asymmetry is established, it should be amplified (and stabilized) by means of appropriate mechanisms.

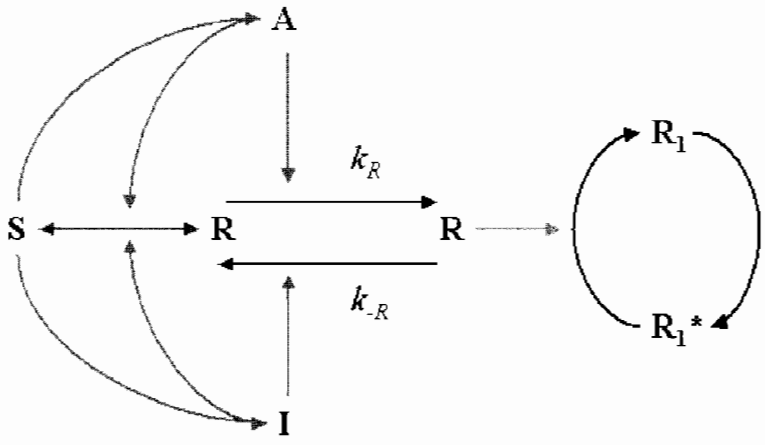

Fig. 5. A kinetic system possessing perfect adaptation that may also provide high gain in the second response element R_1 for a suitable choice of the parameters describing kinetic rates. See the Appendix in [70] for details. (Adapted form [70].)

In [98] a dynamical model is introduced to describe the setting of a rapid initial asymmetry as that described above. This is done as follows. First, a three-state characterization of the membrane is introduced: quiescent (with density ρ_q), activated (density ρ_a) and inhibited (density ρ_i). Since the total density has to be conserved, $\rho_q + \rho_a + \rho_i = 1$. The equations proposed to describe the membrane state are

$$\frac{\partial \rho_q}{\partial t} = -\alpha c \rho_q + \beta_f \rho_i - \beta_i g \rho_q,$$

$$\frac{\partial \rho_a}{\partial t} = \alpha c \rho_q - \delta \rho_a,$$

$$\frac{\partial \rho_i}{\partial t} = -\beta_f \rho_i + \beta_r g \rho_q + \delta \rho_a,$$

which satisfy the previous conservation requirement. Here, α, β_f, β_i, δ and β_r are kinetic constants and c and g respectively denote the concentrations at the membrane of extracellular and intracellular cAMP. These concentrations in turn satisfy

$$\frac{\partial c}{\partial t} = D_c \Delta c - \nu_c c,$$

at the extracellular space, and

$$\frac{\partial g}{\partial t} = D_g \Delta g - \nu_g g,$$

at the intracellular one; ν_c and g_c represent decay terms. It is also assumed that a no-flux condition is satisfied at the boundary

$$D_g \nabla g \cdot \mathbf{n} = D_c \nabla c \cdot \mathbf{n} = 0,$$

where $\mathbf{n}$ denotes the normal at the membrane. The simulations performed in [98] for a suitable choice of parameters (and for equal diffusivities: $D_c = D_g = 2.5 \times 10^{-6}$ cm^2/s) show that asymmetry, characterized in terms of the values of ρ_a, ρ_i is rapidly (less than 1 second) established in the cell (see Figures 2 and 3 in [98]).

We have already remarked on the meaning of adaptation from an engineering point of view. Further discussion on this subject is contained in [120], where the authors recall that there are two ways of constructing systems exhibiting perfect adaptation. The first possibility requires, as observed in [120], fine-tuning the parameters in the corresponding model, an approach consistently followed in the works described so far. A second alternative consists in designing specific structures that create such property inherently. In this vein, adaptation may be viewed as a solution for a common problem in engineering, namely that of designing systems that (quickly) converge toward a specific steady-state output.

A standard solution to this problem is integral feedback control. In its simplest setting, this process can be described by the equations

$$\dot{x} = y, \tag{98}$$

$$y = y_1 - y_0 = k(u - x) - y_0, \quad k > 0. \tag{99}$$

In (98), (99) a process is represented that takes u as an input and produces the output y_1. This process is characterized by constant k in (99). We denote by y the difference between y_1 and the steady-state output y_0. This represents the system error, whose time integral x is fed back into the system, with the aim of obtaining the desired result

$$y(t) \to 0 \quad \text{as } t \to \infty. \tag{100}$$

As recalled in [120], for linear systems a necessary and sufficient condition for robust asymptotic tracking is that the system had integral feedback, as that described by (98).

As observed in [120], an interesting example where these ideas can be applied is the case considered in [6]. These authors derived a two-state (active or inactive) model of a receptor complex, constituted by a receptor and *CheA* and *CheW* proteins, in bacterial chemotaxis. The system output was the concentration of active receptor complexes. A remarkable fact stressed in [6] is that perfect adaptation is achieved as an intrinsic property of the signaling network considered, independently of the kinetic parameters involved. It was then shown in [120] (supplementary material) that a system of differential equations can be written for the biochemical network described in [6] such that, after suitable manipulation, an equation characteristic of integral control is derived. The activity of the system is then shown to asymptotically converge to a fixed steady-state value (cf. (1) in [120]). As the authors of [120] point out, knowing that integral control underlies the robustness of perfect adaptation in the model designed in [6] has significant implications. In particular, it allows for assessing the relevance of any of the several assumptions made in that model. A discussion

on this subject can be found in [120], and the reader is referred to that work for further details on that issue.

3. Some mathematical problems arising from the study of *Dictyostelium discoideum*

It has been already recalled at the Introduction of this chapter that chemotaxis was proposed as a hypothesis in connection with the process of neural wiring in the field of Neuroscience. This last has proved to be a fertile ground in Biology during the XX century, and has exerted a considerable influence in the evolution of other disciplines as Mathematics and Physics. This situation is likely to continue, even at an increased pace, during the foreseeable future. A discussion on current and future research directions at the interface between Mathematics, Neuroscience and Physics can be found in the monograph [116] and references therein.

At a different level of complexity, a relevant role in the blossom of Developmental Biology started at the beginning of the last century has been played by the study of animal models, particularly (but by no means exclusively) those made on the bacteria *E-coli* and the slime mold *Dictyostelium discoideum* (*Dd*). In both cases chemotaxis is a central topic when describing developmental and social life properties of such microorganisms. The reader is referred to [10] for a recent description of current understanding of *E-coli* from a multidisciplinary point of view.

In this section we shall focus on *Dd*, and will discuss some of the mathematical approaches that have been proposed to deal with quantitative problems motivated by the study of such organism. More precisely, the plan of this section is as follows. In Section 3.1 we shortly review some basic facts concerning the biology of *Dd*. Particular attention will be paid to the role played by a chemical messenger (cAMP) in starvation-induced aggregation into some condensation centers, a remarkable feature of *Dd* colonies which has triggered large attention in the biology community. We then focus in Section 3.2 into a particular set of differential equations (the so-called Keller–Segel system) which was initially proposed as a model to describe early stages of aggregation in *Dd* cell cultures, and has been extensively studied by mathematicians since, due to the nontrivial structure displayed by their solutions. In that paragraph the emphasis is therefore on the mathematics, keeping however an eye on the biological motivations. As everywhere in this work, the style will be descriptive, and reference will be made to appropriate articles for details on the underlying mathematical arguments.

While the Keller–Segel (KS) model described in Section 3.2 is of a macroscopic nature, the problem of relating observable macroscopic behavior in *Dd* cultures to individual cell properties has sparked interest in deriving KS equations from microscopic considerations, a multiscale problem of considerable importance, which will be dealt with in Section 3.3. It should be stressed that the considerations to be recalled there are by no means limited to the case of *Dictyostelium*, but rather point at the deep, general question of relating macroscopic properties of organic ensembles (swarms, tissues, organs, ...) to the individual signal exchange and transduction pathways of their members.

We then conclude this section with a discussion on some aspects of pattern formation in *Dd* colonies, particularly in the case of monolayer cultures that can be represented by

two-dimensional (in space) domains. Specifically, we concentrate on early stages of aggregation, and in particular in the occurrence of target and spiral waves and the transition from prevalence of one type of pattern to the other. In mathematical terms, this leads to the question of characterizing reaction–diffusion systems that are able to exhibit that type of traveling waves, a subject which is quickly addressed therein. Once again, understanding the observed dynamic transition from a target- to spiral-dominated scenario seems to call for a multiscale approach which is only at its beginning yet.

3.1. *The social life of Dictyostelium discoideum in a nutshell*

There is a number of recent reviews on *Dd* where the biology of this species is described in detail (cf., for instance, [23,34,48,115]). For definiteness, we shall recall below only a few aspects of that topic which are particularly relevant as background for the mathematical models to be mentioned later.

The basic features of individual and collective behavior in *Dd* colonies are best summarized in the words of John Bonner ([16], p. 62) as follows:

> ... Cellular slime molds are soil amoebae. They feed as separate individuals on bacteria, and after they have finished the food supply, they stream together to central collection points to form a multicellular individual of thousands of cells. ...

In fact the cells migration toward aggregation centers (the "central collection points" in the quotation above) is mediated by a chemical compound (adenosine 3′,5′-cyclic monophosphate, cAMP; cf. [59]) which is produced by cells at the aggregation centers in a pulsatile way upon starvation, and spreads by diffusion [75]. Moreover, *Dd* cells are able to relay the cAMP signal received, thus keeping a cAMP flow in the medium that, when observed through darkfield microscopy, gives raise to fields of circular and spiral waves (for a review, see [48]). This cAMP-mediated chemotactic migration eventually results in the formation of mounds or condensates which, most remarkably, have a rather constant size [99].

Once mounds have been formed, differentiation of mound cells into two cell types (prespore and prestalk) begins. Prestalk cells then migrate to the upper part of the mound to form a tip, whereas prespore cells remain in the lower side of the mound. The object thus formed then elongates to produce a finger-like structure. Subsequent development can unfold in two different ways, as recalled in Figure 6. The first case occurs under favorable environmental conditions, and consists in finger development at the place where it was formed. Prestalk cells, that were situated at the top of the structure, migrate through the prespore cells in the direction of the substratum. Meanwhile, these cells differentiate into stalk cells and die at the end of the process. The growth of the stalk, where prestalk cells are continuously added at its top, goes in parallel with the upward movement of prespore cells, that rise from the substratum to eventually form a ball of cells on top of the stalk (the sorus). Prespore cells in the sorus eventually become spores surrounded by a hard shell, that remain viable for weeks. Germination of spores leads to a new cell cycle for the resulting amoebae.

If conditions are unfavorable, a longer developmental program can be selected. Then the finger structure falls on the substrate and a migratory structure (the slug) is formed,

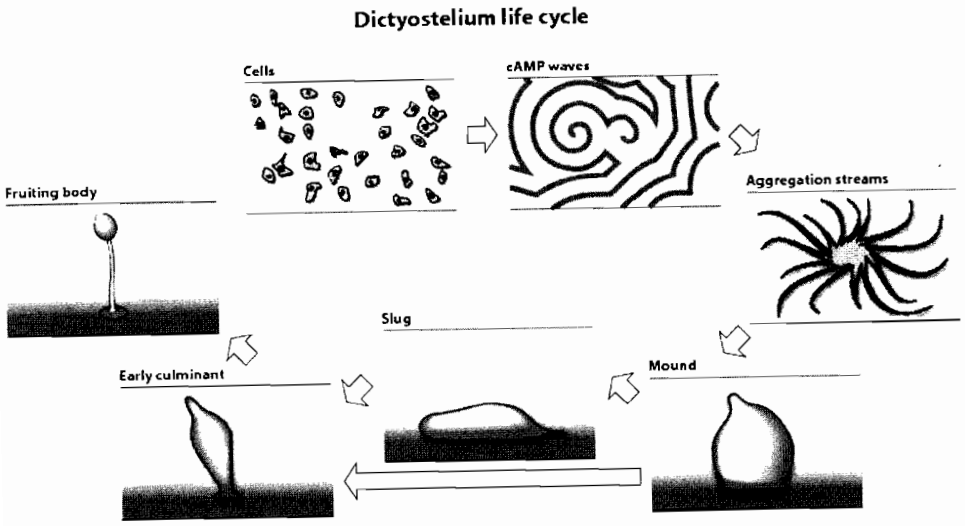

Fig. 6. Evolution of *Dd* cultures after starvation. (Reproduced with permission from [48].)

where prestalk cells are located at the front and prespore cells at the back. Slugs can move toward places more suitable to complete development. When this happens, the slug stops, rounds up and migration of prestalk and prespore cells in opposite direction occurs as in the previous case, after which culmination takes place in the same manner.

3.2. *Early aggregation stages: the Keller–Segel model*

Out of the many mathematical models that have been proposed to deal with particular aspects of chemotaxis, that proposed by Keller and Segel in 1970 (cf. [57]) has received particular attention. There are a number of features on it that can possibly explain the interest it has raised among the mathematical community (witnessed, for instance, by the thorough survey [51] and the monograph [111]). For instance, the model has a very simple structure, reflecting the fact that the underlying hypotheses are reduced to a bare minimum. Moreover, the mathematical analysis of their solutions is nontrivial, and has led to developments of considerable interest. However, the model has proved to be fairly less popular among biologists interested in chemotaxis. Some thoughts on that matter, due to one of the authors of [57], can be found in [56], Chapter 1. See also [41] for a number of interesting remarks on the role of modeling in Biology.

The systems considered in [57] were intended to describe the early aggregation properties of the slime mold *Dictyostelium discoideum*. In particular, the question of the formation of condensates where *Dd* cells gather upon starvation, was paramount there. The authors' approach was neatly explained by them at the Introduction of their work:

> ... By analogy with many problems in the physical world, aggregation is viewed as a breakdown of stability caused by intrinsic changes in the basic parameters that characterize the system ...,

a statement which bears resemblance with that made by Turing in [114]:

> ... A system of chemical substances... although it may originally be quite homogeneous, may later develop a pattern or structure due to an instability of the homogeneous equilibrium, which is triggered off by random disturbances ....

Let us briefly recall the analysis done in [57] for the simplest model considered there. Let $u(x, y, t)$, $v(x, y, t)$ respectively denote the concentrations of amoebae and cAMP in a two-dimensional medium, which can be thought of as an approximate setting for monolayer *Dd* culture in Petri dishes. Then u and v are required to satisfy

$$\frac{\partial u}{\partial t} = -\nabla(D_1 \nabla v) + \nabla(D_2 \nabla u), \tag{101}$$

$$\frac{\partial u}{\partial t} = D_v \Delta v - k(v)v + uf(v), \tag{102}$$

where

$$k(v) = \frac{k_1}{1 + kv}, \tag{103}$$

for some constants $k_1 > 0$ and $k > 0$. In this system, the right-hand side in (101) includes the contributions to time-change of u due to convective motion induced by cAMP and diffusion respectively. In particular, $D_1 = D_1(u, v) > 0$ represents a measure of the influence of the cAMP gradient on the flow of amoebae, and $D_2 = D_2(u, v) > 0$ is a diffusion coefficient corresponding to random motion of *Dd* cells. The right-hand side in (102) has a diffusion term for cAMP (with diffusion coefficient $D_v > 0$), a decay term for that chemical (with kinetic parameter $k(v)$ given in (103)) and a source term, which corresponds to the assumption that cAMP is produced by the cells themselves. In this last case, the kinetic parameter is given by $f(v)$ in (102) and is of a general form. To make up for a well-posed mathematical problem, equations (101)–(103) need to be supplemented with initial values and boundary conditions. When the problem is considered in a bounded domain $\Omega \subset \mathbb{R}^2$, these last are usually taken to be of no-flux type, namely

$$\frac{\partial u}{\partial n} = \frac{\partial v}{\partial n} = 0 \quad \text{at } \partial\Omega, \tag{104}$$

where $\partial\Omega$ denotes the boundary of Ω, and n stands for the (outer) normal at $\partial\Omega$.

A particular type of solution to (101)–(103) are equilibria, defined by

$$u = u_0, \qquad v = v_0 \quad \text{with } u_0 f(v_0) = k(v_0)u_0, \tag{105}$$

provided that the last equation in (105) admits constant roots. A relevant contribution in [57] consists in obtaining conditions under which the steady state (u_0, v_0) in (105) is unstable under perturbations. This instability is thus seen as the first step toward the formation of a condensate. The previous goal is achieved by means of a classical linear stability argument, that is summarized as follows. Set

$$u = u_0 + \bar{u}(x, y, t), \qquad v = v_0 + \bar{v}(x, y, t), \quad |\bar{u}| \ll u_0, |\bar{v}| \ll v_0. \tag{106}$$

Plugging (106) into (101), (102) and neglecting higher-order terms, $\bar{u}$ and $\bar{v}$ are shown to satisfy the linear system

$$\frac{\partial \bar{u}}{\partial t} = -D_1(u_0, v_0)\Delta\bar{v} + D_2(u_0, v_0)\Delta\bar{u}, \tag{107}$$

$$\frac{\partial \bar{v}}{\partial t} = D_v\Delta\bar{v} - \bar{k}\bar{v} + u_0 f'(v_0)\bar{v} + f(v_0)\bar{u}, \tag{108}$$

where $\bar{k} = k(v_0) + v_0 k'(v_0)$. Assuming for simplicity that (107), (108) is satisfied in the whole plane $\mathbb{R}^2$, and trying there

$$\bar{u} = \hat{u}\cos(q_1 x + q_2 y)\,\mathrm{e}^{\sigma t}, \qquad \bar{v} = \hat{v}\cos(q_1 x + q_2 y)\,\mathrm{e}^{\sigma t}, \tag{109}$$

for some constants $\hat{u}$, $\hat{v}$, q_1, q_2 and σ, one readily obtains

$$(F - \sigma)\hat{v} + f(v_0)\hat{u} = 0, \qquad D_1 q^2 \hat{v} - \big(D_2 q^2 + \sigma\big)\hat{u} = 0,$$

where $q^2 = q_1^2 + q_2^2$ and $F \equiv f'(v_0)u_0 - \bar{k} - q^2 D_2$, and D_1, D_2 are evaluated at (u_0, v_0). The previous system has a nontrivial solution provided that

$$\sigma^2 - \sigma\big(F - q^2 D_2\big) - \big(q^2 f(v_0) D_1 + q^2 D_2 F\big) = 0. \tag{110}$$

Analysis of this quadratic equation shows that the corresponding roots are real, and the condition for obtaining values $\sigma > 0$ is that

$$\frac{D_1 v_0}{D_2 u_0} + \frac{u_0 f'(v_0)}{\bar{k}} > 1. \tag{111}$$

Summing these results up, we have seen that (111) is required for σ to be positive in (109), so that the corresponding oscillatory perturbation of the steady state tends to increase in amplitude for small times. However, this argument does not imply that such a perturbation will increase for ever. Indeed, as $\bar{u}$ and $\bar{v}$ in (109) grow larger, the higher-order terms which were discarded in (107), (108) become relevant, and the previous argument no longer applies. Thus a fully nonlinear analysis for intermediate times is required in order to examine the formation of condensates.

A first step in that direction was later provided by Nanjundiah (cf. [82]). He considered a simplified version of (101), (102), namely

$$\frac{\partial u}{\partial t} = \nabla(D_u \nabla u - \chi u \nabla v), \tag{112}$$

$$\frac{\partial v}{\partial t} = D_v \Delta v + Au - Bv \tag{113}$$

(the so-called gradient proportional chemotaxis in [82]), where the diffusion coefficients D_u and D_v, and parameters χ, A and B are positive constants. Incidentally, this system is commonly referred to as the Keller–Segel system in the mathematical literature.

Nanjundiah proposed that condensate formation in *Dd* monolayer cultures would correspond to blow-up in finite time T for (112), (113), in such a manner that a Dirac-delta type singularity will develop as the blow-up time is approached:

$$u(x,t) \to M\delta(x - x_0) \quad \text{for some } M > 0 \text{ and some } x_0 \text{ as } t \to T, \tag{114}$$

a property commonly referred to as the onset of a chemotactic collapse. We remark on pass that equations (112), (113) can be made dimensionless upon the change of variables:

$$u \to u^* = \frac{A\chi}{BD_u}u, \qquad v \to v^* = \frac{\chi}{D_u}v, \qquad r \to r\sqrt{\frac{B}{C_v}}, \qquad t \to Bt, \tag{115}$$

which transforms (112), (113) into

$$\frac{\partial u^*}{\partial t} = D\nabla\big(\nabla u^* - u^*\nabla v^*\big), \quad D = \frac{D_u}{D_v}, \tag{116}$$

$$\frac{\partial v^*}{\partial t} = \Delta v^* + u^* - v^*. \tag{117}$$

Notice that in this case the instability condition (111) reads

$$u^*(x, 0) > 1, \tag{118}$$

which suggests that the uniform distribution is unstable above a critical concentration of amoebae. Further analysis was later done in [22], where it was shown that no blow-up occurs in finite time for (112), (113) in space dimension $N = 1$, and in [21] where an asymptotic argument was presented to show that, in space dimension $N = 2$ chemotactic collapse will occur if the cell's density goes above some threshold. More precisely, the statement in [21] goes as follows. Consider radial solutions of (112), (113) in a ball $B_L = \{(x, y)\colon x^2 + y^2 < L^2\}$, and introduce new variables given by

$$\tilde{u} = \frac{A\chi L^2}{D_u D_v}u, \qquad \tilde{v} = \frac{\chi}{D_u}v, \qquad \rho = \frac{r}{L}, \qquad \tau = \frac{D_u t}{L^2}. \tag{119}$$

In these new dimensionless variables, (112), (113) is changed into

$$\frac{\partial \tilde{u}}{\partial \tau} = \frac{1}{\rho}\frac{\partial}{\partial \rho}\left(\rho\left(\frac{\partial \tilde{u}}{\partial \rho} - \tilde{u}\frac{\partial \tilde{v}}{\partial \rho}\right)\right),$$

$$\delta_1 \frac{\partial \tilde{v}}{\partial \tau} = \tilde{u} - \delta_2 \tilde{v} + \frac{1}{\rho}\frac{\partial}{\partial \rho}\left(\rho\frac{\partial \tilde{v}}{\partial \rho}\right),$$

where now $0 < \rho < 1$, and

$$\delta_1 = \frac{D_u}{D_v}, \qquad \delta_2 = \frac{BL^2}{D_v}. \tag{120}$$

Then, in the limit where $0 < \delta_1 < 1$ and $0 < \delta_2 < 1$, a formal argument is provided in [21] that shows that for chemotactic collapse to occur, one needs

$$\int_0^1 \rho\tilde{u}(\rho, 0)\,\mathrm{d}\rho > 4.$$

When written in terms of the original variables in (112), (113), this condition reads

$$M_0 \equiv \int_{B_L} u_0(x, y)\,\mathrm{d}x\,\mathrm{d}y > \frac{8\pi D_u D_v}{A\chi}. \tag{121}$$

The previous argument hints at a threshold result for chemotactic collapse when $N = 2$. Namely, when (112), (113) are considered with no-flux conditions (104), so that the cell population is preserved,

$$\int_{B_L} u(x, y, t)\,\mathrm{d}x\,\mathrm{d}y = \int_{B_L} u_0(x, y)\,\mathrm{d}x\,\mathrm{d}y,$$

as long as the solution exists, we expect that the value

$$M^* = \frac{8\pi D_u D_v}{A\chi} \tag{122}$$

will play a critical role, in that solutions should be global in time for $M_0 < M^*$ (M_0 being as in (121)) and condensates of Dirac-delta type should form when $M_0 > M^*$. As it turns out, this happens to be the case when radial solutions are considered. Moreover, whenever blow-up occurs at an interior point for (112), (113), it has to correspond to chemotactic collapse at that point (cf. (114)) with $M = M^*$. We refer to the reader to [51] for a detailed account of the precise statements concerning global existence and blow-up for (112), (113) as well as for exhaustive references (up to 2003) of the works where such results were obtained. Among these last we should merely mention here the articles [12,49,54,80] and [81] as illustrative of the different techniques developed to derive the results just sketched.

At this juncture, it is worth to mention that chemotactic collapse (as described in (114)) is known to be the only possible type of singularity formation in space dimension $N = 2$ for system (112). However, when $N = 3$ a different type of hydrodynamic collapse has been shown to occur in [47] for a simplified version of (112) in the whole space.

We conclude this section with some remarks on recent developments motivated by (or related to) systems akin to (112)–(113). It goes without saying that reference to the works that follow is far from being complete, and the reader will find additional information by consulting the articles mentioned. To begin with, the occurrence of singularities for models similar to (112), (113) has been recently examined in [13,14] in the critical case when $M_0 = M^*$ (cf. (121), (122)). Global existence results for equations of Keller–Segel type have been derived in [24], whereas an outline of PDE models (parabolic and hyperbolic) to describe chemotaxis can be found in [92]. Recently, systems of Keller–Segel type with nonlinear diffusivities have been considered by a number of authors, among which we

should mention [109,110] and [72]. Back to the original KS model, where blow-up is taken as a fingerprint for aggregation in mounds, a natural question consists in ascertaining in which sense (if any) solutions can be continued after condensate formation. This issue has been addressed in [117,118].

3.3. *The Keller–Segel model revisited: from micro to macro*

The system (101)–(103), as well as the variants thereof considered in [57], were obtained by means of macroscopic (and largely heuristical) considerations. It has been shown, however, that equations of this type can be derived starting from microscopic models, much in the same way as the linear diffusion equation can be arrived at as a macroscopic limit for random walks (cf., for instance, [9]). We next recall various manners in which macroscopic chemotaxis equations can be obtained from microscopic models.

(I) *Chemotaxis and biased random walks.* Next we shall borrow from [86] and [87], and quickly review how to derive a chemotaxis model from a master equation for a continuous in time, discrete in space random walk on a one-dimensional lattice. To this end, let us define $u_i(t)$ as the probability of a walker to be at an (integer) point i at time t, starting from $i = 0$ at $t = 0$. Assume now that the random walk evolves according to the equation

$$\frac{\partial u_i}{\partial t} = T_{i-1}^+ u_{i-1} + T_{i+1}^- u_{i+1} - \big(T_i^+ + T_i^-\big)u_i, \tag{123}$$

where $T_i^\pm(\cdot)$ denote the transitional probabilities per unit time of a one-step jump to $i \pm 1$. To account for chemotaxis, a spatial bias is introduced, so that one writes $T_i^\pm = T_i^\pm(v)$, where v denotes the chemical concentration in the lattice. If we assume that cells can detect a local gradient, we may write

$$T_i^\pm = \alpha + \beta\big(\tau(v_{i\pm1}) - \tau(v_i)\big), \tag{124}$$

where α and β are positive parameters, and $\tau(\cdot)$ is a function which depends on the particular mechanism for signal detection being considered. Plugging (124) into (123), one readily obtains

$$\begin{aligned}\frac{\partial u_i}{\partial t} &= \alpha(u_{i+1} - 2u_i + u_{i-1}) \\ &\quad - \beta\big((u_{i+1} + u_i)\big(\tau(v_{i+1}) - \tau(v_i)\big) - (u_i + u_{i-1})\big(\tau(v_i) - \tau(v_{i-1})\big)\big).\end{aligned}$$

We then set $x = ih$, and consider x as a continuous variable. We also postulate that the transitional probabilities change according to the scaling $T_h^\pm = (k/h^2)T^\pm$ for some $k > 0$. On extending the definition of u_i in a corresponding manner, and neglecting terms of order $O(h^2)$, one eventually arrives at

$$\frac{\partial u}{\partial t} = D_u \frac{\partial^2 u}{\partial x^2} - \frac{\partial}{\partial x}\left(u\chi(v)\frac{\partial v}{\partial x}\right), \tag{125}$$

where

$$D_u = k\alpha, \qquad \chi(v) = 2k\beta \frac{d\tau(v)}{dv}$$

(compare with (101)). Notice that no mechanism for generation of the chemical species has been proposed as yet. A simple way of addressing this issue consists in coupling (125) with a phenomenological equation

$$\frac{\partial v}{\partial t} = D_v \frac{\partial^2 v}{\partial x^2} + g(u, v) \tag{126}$$

for some $D_v > 0$ and some kinetic function $g(u, v)$ (compare with (102)). We remark on pass that it is easy to incorporate counting mechanisms in the model that limit the size of the aggregates. For instance, arguing as in [87] we may replace (124) by

$$T_i^{\pm} = q(u_{i\pm1})\big(\alpha + \beta\big(\tau(v_{i\pm1}) - \tau(v_i)\big)\big), \tag{127}$$

which amounts to assume that the probability of jumping into a neighboring site depends on the space actually available there. For instance, a possible choice for $q(u)$ is

$$q(u) = 1 - \frac{u}{u_{\max}} \quad \text{for } 0 < u < u_{\max}.$$

When we repeat the previous argument with (124) replaced by (127), we readily see that (125) has to be replaced by

$$\frac{\partial u}{\partial t} = \frac{\partial}{\partial x}\left(D_u\big(q(u) - q'(u)u\big)\frac{\partial u}{\partial x} - q(u)u\chi(v)\frac{\partial v}{\partial x}\right). \tag{128}$$

We point out that the existence of attractors for systems of the type (126), (128) has recently been proved in [119].

In the context of our current discussion on global existence vs blow-up for Keller–Segel type systems, it is worth remarking on work conducted on a related model, which has been used to describe vasculogenesis (cf. [4,37]) and reads as follows:

$$\begin{aligned}
&\frac{\partial n}{\partial t} + \nabla(n \cdot v) = 0,\\
&\frac{\partial v}{\partial t} + v\nabla v = \mu\nabla c - \beta v - \nabla g(n),\\
&\frac{\partial c}{\partial t} = D\Delta c + \alpha n - \frac{c}{\tau},
\end{aligned} \tag{129}$$

where n and c denote the concentrations of cells and chemoattractant respectively, and v stands for the cell velocity. The equations above take into account cell migration and

chemotaxis (μ measuring the strength of the cell response), friction with substratum (parameter β) and pressure exerted by cells (represented by $g(n)$). As to D, α and τ they respectively represent the diffusion coefficient of the chemical, its production rate and a characteristic degradation time. Neglecting persistence (that is, the inertial term) in the second equation, one obtains

$$0 = \mu\nabla c - \beta v - \nabla g(n)$$

or

$$v = \chi\nabla c - \nabla h(n),$$

with $\chi = \mu/\beta$, $h(n) = 1/\beta g(n)$. Plugging the equation just derived for v into the mass balance equation above, one eventually obtains

$$\begin{aligned}
&\frac{\partial n}{\partial t} = \nabla\big(n\nabla h(n) - \chi n\nabla c\big),\\
&\frac{\partial c}{\partial t} = D\Delta c + \alpha n - \frac{c}{\tau},
\end{aligned}$$

which is of the Keller–Segel type previously considered. It has been shown in [60] that for functions $h(n)$ that increase fast enough blow-up cannot occur. Previously, a stability analysis of homogeneous solutions to the full system (129) was done in [61]. In particular it was shown that the effect of pressure controls possible instabilities at low densities, thus preventing initiation of blow-up.

(II) *Chemotaxis and velocity jump processes.* Velocity-jump processes are a particular type of stochastic processes, which roughly speaking can be described as consisting in a sequence of runs, separated by reorientations, where a new velocity is chosen (cf. [83] for a detailed discussion). In mathematical terms, they lead to the consideration of Boltzmann equations, namely

$$\frac{\partial p}{\partial t} + \nabla_x vp = -\lambda p + \lambda \int T\big(v, v'\big)p\big(x, t, v'\big)\,dv'. \tag{130}$$

Here $p(x, v, t)$ denotes the density function in a $2n$-dimensional space with coordinates $x \in \mathbb{R}^n$ (representing the position of an individual) and $v \in \mathbb{R}^n$ (describing its velocity). In this way, $p(x, v, t)\,dx\,dv$ gives the number density of individuals whose position is located between $(x, x + dx)$, and whose velocity lies within $(v, v + dv)$. In (130) it is assumed that the random velocity changes follow a Poisson process of intensity λ, so that λ^{-1} is the mean run length time between random choices of direction. On the other hand, the kernel $T(v, v')$ represents the probability of a velocity change v' to v, and $\int T(v, v')\,dv = 1$ for any v.

The derivation of systems as (101), (102) from equations of the type (130) has been discussed by several authors (see, for instance, [18,50,84], etc.). Here we shall remark

on a suitable extension of the approach in [50,84] which has been introduced by Erban and Othmer [32,33] and where dependence on internal cell kinetics, as that recalled in Section 2.6, is taken into account; see also [7] and [8] for a detailed discussion on related multiscale topics.

The authors of [32], [33] assume that the density of the biological population being considered $p(x, v, y, t)$ depends also on an internal state $y \in \mathbb{R}^m$, $m \geqslant 1$, which is supposed to follow the kinetics given by a system of the form

$$\frac{\mathrm{d}y}{\mathrm{d}t} = f(y, S), \tag{131}$$

where $y = (y_1, \ldots, y_m)$ denotes the internal variables or species, $S(x,t) = (S_1, \ldots, S_d) \in \mathbb{R}^d$ corresponds to the chemical cues acting in the environment, and f represents the precise internal dynamics of the process (for a particular choice of f, see [107]). In addition, the mean run length is also assumed to depend on y. In this way, (130) is to be replaced by

$$\frac{\partial p}{\partial t} + \nabla_x v p + \nabla_y f p = -\lambda(y) p + \int \lambda(y) T\big(v, v', y\big) p\big(x, t, v', y\big)\, \mathrm{d}v'. \tag{132}$$

A perturbative analysis performed in [32,33] shows that, to the lowest order, the cell variable

$$n(x,t) = \iint p(x, t, v, z)\, \mathrm{d}v\, \mathrm{d}z$$

satisfies the equation

$$\frac{\partial n}{\partial t} = \nabla\big(D\nabla n - n\chi(S)\nabla S\big), \tag{133}$$

provided that a number of assumptions are made. In particular, the internal dynamics is assumed to be described by two variables y_1, y_2 which represent excitory and inhibitory mechanisms respectively. Furthermore, $S = S(x)$ is taken to be independent of time. In equation (133), D and χ are respectively the diffusion and chemosensitivity tensors, so that an equation of type (101) is recovered in the isotropic case.

(III) *Chemotaxis equations as limits of stochastic many-particle systems.* The next approach to be succinctly reviewed here is due to Stevens [108] who considered a population of N units or particles, formed by microorganisms (labeled u) and a chemical produced by them (labeled v), so that $S(N,t) = S_u(N,t) + S_v(N,t)$ denotes the total number of particles in the system at time t. Let $P_N^k(t)$ describe the position of the kth particle ($k \in S(N,t)$) at time t. In [108] the following empirical processes are considered:

$$t \to S_{N_u}(t) = \frac{1}{N} \sum_{k \in S_u} \delta_{P_N^k(t)}, \qquad t \to S_{N_v}(t) = \frac{1}{N} \sum_{k \in S_v} \delta_{P_N^k(t)},$$

where δ_x denotes Dirac's delta at $x \in \mathbb{R}^d$, $d \geqslant 1$. A key assumption in [108] is that the dynamics of each particle depends on the configuration of other particles in a neighborhood around it, and as $N \to \infty$, the interaction of particles is rescaled in a moderate way (cf. Section 2 in [108]). On introducing smoothed versions of $S_{N_i}(t)$, $i = u, v$, of the form $\widehat{S_{N_i}}(t,x) = (S_{N_i}(t) * W_N * \widehat{W}_N)(x)$ for some probability densities W_N, $\widehat{W}_N$ satisfying a suitable scaling assumption (which provides a precise meaning to the assumption on moderate interaction), a system of stochastic differential equations is written for the particle populations (cf. Section 3 in [108]). Using Ito's formula (cf., for instance, [38,116]), one eventually obtains for any regular test function f,

$$\begin{aligned}
&\big\langle S_{N_u}(t), f\big\rangle \\
&\quad = \frac{1}{N} \sum_{k \in S_u} f\big(t, P_N^k(t)\big) \\
&\quad = \big\langle S_{N_u}(0), f(0,\cdot)\big\rangle \\
&\qquad + \int_0^t \Big\langle S_{N_u}(s), \chi_N(s,\cdot)\nabla \hat{s}_{N_v}(s,\cdot)\nabla f(s,\cdot) + \mu \Delta f(s,\cdot) + \frac{\partial}{\partial s} f(s,\cdot)\Big\rangle \mathrm{d}s \\
&\qquad + \frac{1}{N} \int_0^t \sum_{k \in S_u} \sqrt{2\mu}\nabla f\big(s, P_N^k(s)\big)\, \mathrm{d}W^k(s),
\end{aligned} \tag{134}$$

$$\begin{aligned}
&\big\langle S_{N_v}(t), f\big\rangle \\
&\quad = \big\langle S_{N_v}(0), f(0,\cdot)\big\rangle \\
&\qquad + \int_0^t \Big\langle S_{N_v}(s), \eta \Delta f(s,\cdot) + \frac{\partial}{\partial s} f(s,\cdot)\Big\rangle \mathrm{d}s \\
&\qquad + \frac{1}{N} \int_0^t \sum_{k \in S_v} \sqrt{2\eta}\nabla f\big(s, P_N^k(s)\big)\, \mathrm{d}W^k(s) + \frac{1}{N} \int_0^t \sum_{k \in S_u} f\big(s, P_N^k(s)\big)\beta_N^{k^*}(\mathrm{d}s) \\
&\qquad - \frac{1}{N} \int_0^t \sum_{k \in S_v} f\big(s, P_N^k(s)\big)\gamma_N^{k^*}(\mathrm{d}s).
\end{aligned} \tag{135}$$

In equations (134), (135) it is assumed that any particle $k \in S_u(N,t)$ at position $P_N^k(t)$ at time t may produce a particle $k^* \in S_v(N,t)$ with intensity $\beta_N(t, P_N^k(t))$, where $\beta_N(t,x) = \beta(\hat{s}_{N_u}(t,x), \hat{s}_{N_v}(t,x))$. This reflects the assumption that chemoattractant is produced by the chemotactic cells themselves. On the other hand, any particle $k \in S_v(N,t)$ may decay with a coefficient $\gamma_N(t, P_N^k(t)) = \gamma(\hat{s}_{N_u}(t,x), \hat{s}_{N_v}(t,x))$. On its turn, $\chi_N(t, P_N^k(t)) = \chi(\hat{s}_{N_u}(t,x), \hat{s}_{N_v}(t,x))$ is a chemosensitivity term arising from the stochastic equation

$$\mathrm{d}P_N^k(t) = \chi_N\big(t, P_N^k(t)\big)\nabla \hat{s}_{N_v}\big(t, P_N^k(t)\big)\, \mathrm{d}t + \sqrt{2\mu}\, \mathrm{d}W^k(t),$$

where $W^k(\cdot)$ are independent Brownian movements. Finally, $\eta > 0$ and $\mu > 0$, and $\beta_N^{k^*}(\sigma)$ and $\gamma_N^{k^*}(\sigma)$ are taken to be Poisson-type point processes (cf. Section 3 in [108]).

Under a number of technical assumptions, it was proved in [108] that one can pass to the limit in (134), (135) as $N \to \infty$, to eventually obtain the following limit equations:

$$\begin{aligned}
&\langle u(t,\cdot), f(t,\cdot)\rangle \\
&\quad = \langle u_0(\cdot), f(0,\cdot)\,ds\rangle \\
&\qquad + \int_0^t \langle u(s,\cdot), \chi_\infty(s,\cdot)\nabla v(s,\cdot)\nabla f(s,\cdot)\,ds\rangle \\
&\qquad + \int_0^t \left\langle u(s,\cdot), \mu\Delta f(s,\cdot) + \frac{\partial}{\partial s} f(s,\cdot)\right\rangle ds, \\
&\langle v(t,\cdot), f(t,\cdot)\rangle \\
&\quad = \langle v_0(\cdot), f(0,\cdot)\,ds\rangle \\
&\qquad + \int_0^t \left\langle v(s,\cdot), \mu\Delta f(s,\cdot) + \frac{\partial}{\partial s} f(s,\cdot) - \gamma_\infty(s,\cdot) f(s,\cdot)\,ds\right\rangle \\
&\qquad + \int_0^t \langle u(s,\cdot), \beta_\infty(s,\cdot) f(s,\cdot)\rangle ds,
\end{aligned}$$

where $\chi_\infty(\tau, x) = \chi(u(x,t), v(x,t))$ and a similar definition is made for β_∞, γ_∞. These equations can be considered as a weak form of

$$\begin{aligned}
\frac{\partial u}{\partial t} &= \mu\Delta u - \nabla\big(\chi(u,v)\nabla v\big), \\
\frac{\partial v}{\partial t} &= \eta\Delta u + \beta(u,v)u - \gamma(u,v)v,
\end{aligned}$$

which is of Keller–Segel type (cf. (101), (102)).

3.4. *Pattern formation in Dictyostelium discoideum*

Here we shall comment on some aspects of the starvation-induced aggregation in monolayer colonies of the slime mold *Dd*. This is a well-documented phenomenon, for which a wealth of evidence is available. We shall recall below some key features in that process, and some related mathematical models will be remarked upon.

(I) *The dynamics of aggregation: some facts.* In this paragraph we shall follow the recent survey [48] and describe the early stages of aggregation in sequential order. The aggregation process induced by food exhaustion last for about 8 hours in wild type (WT) *Dd* cultures. For aggregation to start, a minimum cell density (about 2.5×10^4 cells/cm^2) is required. Laboratory experiments are customarily done at much higher densities, of about $4\text{–}65 \times 10^4$ cells/cm^2. When the process starts, a few cells, which are supposed to be at a comparatively advanced stage of their own cell cycle, begin to emit pulses of cAMP in a periodic manner, approximately every 5–6 minutes. Upon reception of the cAMP signal, cells internally produce cAMP, part of which is secreted outside to keep the signaling process going on, thus establishing a feedback loop. In monolayer cultures, cAMP propagation gives raise to target and spiral wave patterns that can be observed by means of darkfield microscopy. Reception of the cAMP signals is followed by migration toward some of the cAMP sources. In doing so, streams of *Dd* cells are formed that converge toward aggregation points. There, a size-regulation process is observed, since aggregates achieve a characteristic size, which depends on the number of cells initially available and the dimensions of the surrounding medium. As condensates are formed, a transition from a bidimensional setting to a three-dimensional one occurs, since cells in the condensates pile up each other to eventually produce solid, full three-dimensional mounds. Formation of the mound is followed by a subsequent stage in the developmental process of the *Dd* colony which will not be considered here.

In the sequence of steps briefly recalled above, a few ones stand out as particularly intriguing. One of those is the onset of circular and spiral waves, and the transition from one type of dynamics to the other. We have mentioned that aggregation starts when a few spots in the colony (each of them possibly containing a reduced number of synchronized cells) begins to emit periodic pulses of cAMP. These are visualized as circular waves, usually termed as targets. Soon after that, darkfield microscopy reveals a coexistence of targets and spiral patterns, and by 5 hours after starvation, spiral wave territories dominate and persist in WT *Dd* colonies. The transition just mentioned is known to depend on a number of parameters. One of them is cell density, since targets dominate for low values, whereas for higher densities the situation is just the opposite. Also, addition of a uniform spray of cAMP has dramatic effects on the nature of the patterns observed, depending on the timing of cAMP supply. For instance, if applied soon after starvation, spirals are temporally suppressed to eventually reappear afterward. However, if the uniform cAMP signal is sprinkled at later times, spirals happen to be suppressed for good, and only targets will remain henceforth (cf. [68,69]; see also [48] for a review of related results). In the sequel we shall concentrate on describing some of the mathematical approaches that have been proposed to account for various aspects of the signaling features just recalled.

(II) *From targets to spirals: mathematical models.* The aggregation picture just sketched raises a number of questions. For instance, one may wonder how target and spiral patterns are generated, and what is the precise manner in which a transition from the first to the second type of waves occurs. These issues have been addressed by a number of authors, in particular by Cox [67,88,101], Goldbeter [66,74] and Othmer [26,85,112] to mention but a few names. While a satisfactory global model for the overall aggregation process has not been obtained as yet, a good deal of knowledge on some particular steps has been already obtained. For this we refer to the aforementioned references as well as to the review [48] where certain of these results are discussed in some detail.

In mathematical terms, a basic preliminary question consists in identifying those reaction–diffusion systems (and the underlying physical assumptions) that admit traveling wave solutions in the form of expanding circles (targets) or spirals. This has been shown to occur both in oscillatory and excitable systems, on which we shortly remark below. To simplify the presentation, we shall confine ourselves to the case of continuous equations,

although discrete models (for instance, of a cellular automaton type) have proven to be quite useful to gain insight into a number of related biological problems. For this last type of techniques, the reader is referred to the recent monograph [30].

Let us briefly remark on terminology. Following [79], we shall consider oscillatory media as a continuous limit of a large population of self-oscillating elements, with (weak) interactions between neighbors due to diffusion. On its turn, excitable media are formed by elements, any of which is able to return to an initial rest state after undergoing a burst of activity triggered by a sufficiently large perturbation, which may be originated by diffusional flow from neighboring elements in the medium. A characteristic of excitable media is that they allow for propagation of pulses, a type of traveling wave which connects the same equilibrium value ahead and behind the wave. Oscillatory and excitable regimes may sequentially develop and coexist in biological systems. We next remark on different aspects of wave propagation in such situations.

A typical model of oscillatory media is provided by the so-called λ–ω systems [52,63] which are of the form

$$\frac{\partial u}{\partial t} = D_1 \Delta u + \lambda(A)u - \omega(A)v, \tag{136}$$

$$\frac{\partial v}{\partial t} = D_2 \Delta v + \omega(A)u + \lambda(A)v, \tag{137}$$

where $D_1, D_2 > 0$, and λ, ω are given functions of $A = (u^2 + v^2)^{1/2}$. On these, conditions are imposed so that the reduced kinetic system (obtained by setting $D_1 = D_2 = 0$) should have a stable limit cycle with amplitude α and frequency $\omega(\alpha)$. When $D_1 = D_2 = D > 0$ in (136), (137) that system may be written in a more compact manner by setting

$$w = u + iv, \tag{138}$$

which yields

$$\frac{\partial w}{\partial t} = (\lambda + i\omega)w + D\Delta w. \tag{139}$$

For instance, in the case considered in [64], $\lambda(a) = \varepsilon - aA^2$, $\omega(a) = c - bA^2$, so that (139) reads

$$\frac{\partial w}{\partial t} = (\varepsilon + ic)w - (a + ib)|w|^2 w + D\Delta w,$$

which can be thought of as a particular type of a Ginzburg–Landau equation (cf. [63] for details on the derivation of that type of models). It is natural to look for solutions of (139) in the form

$$w = Ae^{i\phi}, \tag{140}$$

where A is an amplitude variable and ϕ its corresponding phase. From (139) and (140), it readily follows that A and ϕ should satisfy

$$\frac{\partial A}{\partial t} = A\lambda(A) - DA|\nabla\phi|^2 + D\Delta A, \tag{141}$$

$$\frac{\partial \phi}{\partial t} = \omega(A) + \frac{2D}{A}(\nabla A \cdot \nabla\phi) + D\Delta\phi. \tag{142}$$

At this juncture, it is worth observing that a large class of reaction–diffusion equations can be approximated, in some asymptotic limit, by means of λ–ω systems. For instance, let us follow [43] and consider the equations

$$\frac{\partial A_1}{\partial t} = F_1(\mu, A_1, A_2) + \nabla\big(D_1(\mu, A_1, A_2)\nabla A_1\big), \tag{143}$$

$$\frac{\partial A_2}{\partial t} = F_2(\mu, A_1, A_2) + \nabla\big(D_2(\mu, A_1, A_2)\nabla A_2\big), \tag{144}$$

where μ is a (nondimensional) parameter such that at some value $\mu = \mu_0$ the reduced kinetic equations (obtained by setting $D_1 = D_2 = 0$ above) undergoes a bifurcation from a stable state (A_1^0, A_2^0) to a stable limit cycle: in mathematical terms, a Hopf bifurcation is said to occur. Arguing as in [43], Appendix A, one then assumes $0 < \mu - \mu_0 \ll 1$, and look for solutions of the form

$$A_i \sim A_i^0 + (\mu - \mu_0)^{1/2} A(T, \tilde{x}) a_i \cos\big(\omega t + \gamma_i + \phi(T, \tilde{x})\big), \quad i = 1, 2,$$

where $\tilde{x} = (\tilde{x}_1, \tilde{x}_2) = (\mu - \mu_0)^{1/2}(x_1, x_2)$, a_i and γ_i are suitable constants, and $T = (\mu - \mu_0)t$. Then the amplitude ϕ and phase A are shown to evolve according to

$$\begin{pmatrix} \frac{\partial A}{\partial T} \\ A\frac{\partial \phi}{\partial T} \end{pmatrix} = \begin{pmatrix} \cos z & -\sin z \\ \sin z & \cos z \end{pmatrix} \begin{pmatrix} \Delta A - A|\nabla\phi|^2 \\ A\Delta\phi + 2\nabla A \cdot \nabla\phi \end{pmatrix} + \begin{pmatrix} A(1 - A^2) \\ qA^3 \end{pmatrix}, \tag{145}$$

where q and z are certain constants determined from the original system (143), (144). In particular, when $D_1 = D_2$, then $z = 0$, and a λ–ω system is obtained, namely

$$\frac{\partial A}{\partial T} = \Delta A - A|\nabla\phi|^2 + A\big(1 - A^2\big), \tag{146}$$

$$A\frac{\partial \phi}{\partial T} = A\Delta\phi + 2\nabla A \cdot \nabla\phi + qA^3. \tag{147}$$

We next discuss on spiral patterns. An m-armed ($m \geqslant 1$) spiral wave of (139) is defined as a solution of the form (140) (if any), such that

$$A = A(r), \qquad \phi = \Omega t + m\theta + \psi(r), \tag{148}$$

where (r, θ) are polar coordinates in $\mathbb{R}^2$. A quick check then reveals that A and ψ should then satisfy

$$D\left(A'' + \frac{A'}{r}\right) + A\left(\lambda(A) - D(\psi')^2 - \frac{Dm^2}{r^2}\right) = 0, \tag{149}$$

$$D\left(\psi'' + \left(\frac{1}{r} + \frac{2A'}{A}\right)\psi'\right) = \Omega - \omega(A), \tag{150}$$

a system which is to be supplemented with boundary conditions

$$A(0) = \psi'(0) = 0, \qquad A(r) \to A(\infty) \quad \text{as } r \to \infty. \tag{151}$$

From (149)–(151) it follows at once that

$$\psi'(\infty) = \left(\frac{\lambda(A_\infty)}{D}\right)^{1/2}, \qquad \Omega = \omega(A_\infty).$$

A brief account of early existence results for (149)–(151) can be found in [46]. A rather general existence result has been obtained in [102] (cf. also [35]) that will be described next. Consider the system

$$\frac{\partial u}{\partial t} = D\Delta u + f(u, \mu) \quad \text{for } x \in \mathbb{R}^2, u = (u_1, u_2). \tag{152}$$

Assume that $f(0, \mu) = 0$ for $0 < |\mu| \ll 1$ and that the linearization $\frac{\partial f}{\partial u}(0, 0)$ has a pair of purely imaginary eigenvalues $\pm i\omega_H$, so that the corresponding Hopf bifurcation in the purely kinetic case ($D = 0$) can be written, in suitable variables, in the form

$$\dot{z} = \lambda(\mu)z + \beta z|z|^2 + O(|z|^5) \quad \text{with } \operatorname{Re}\beta < 0. \tag{153}$$

The linearization of (152) around $u = 0$ reads

$$\frac{\partial u}{\partial t} = D\Delta u + \frac{\partial f}{\partial u}(0, 0)u,$$

which after taking Fourier transform yields the dispersion relation

$$d(\lambda, ik) \equiv \det\left(-Dk^2 + \frac{\partial f}{\partial u}(0, 0) - \lambda\right) = 0 \quad \text{for } k \in \mathbb{R}. \tag{154}$$

Then for wavenumbers $k \in \mathbb{R}$ near zero, the eigenvalue $\lambda = i\omega_H$ continues to a spectral curve $\lambda(ik, 0)$ such that $\lambda(0, 0) = i\omega_H$ and

$$\lambda(ik, 0) = i\omega_H + \alpha k^2 + O(k^4). \tag{155}$$

The following result has been proved in [102]. Assume that (i) $\lambda(0, 0) = i\omega_H$ is a simple zero of (154) and the only purely imaginary solution of that equation for any

real k, (ii) $\frac{\partial}{\partial \mu} \operatorname{Re}\lambda(0, 0) > 0$ and for α, β given respectively in (155) and (153) we have $|\arg(\beta/\alpha)| < \delta$ for some $\delta > 0$ sufficiently small. Then for $\mu > 0$ small enough, there exists an Archimedean spiral wave of (152).

By this last we mean a bounded rotating wave solution $q_*(r, \theta - \omega_* t)$ of (152), with some nonzero rotation frequency ω_*, which converges to plane wavetrains in the farfield, that is,

$$\left|q_*(r, \theta) - q_\infty\left(r - \left(\frac{\theta}{k_\infty}\right)\right)\right| \to 0$$

as $r \to \infty$ uniformly for $\theta \in [0, 2\pi]$, for some k_∞.

We now turn our attention to target patterns. These can be roughly described as a wave train of concentric circles propagating from a center, which is often termed as a pacemaker. Following [42], we shall look for targets in reaction–diffusion systems of the type

$$\frac{\partial A}{\partial t} = F(A) + \varepsilon D\Delta A + \varepsilon g(x, A), \tag{156}$$

where $A = (A_1, A_2)$, $D > 0$, $0 < \varepsilon \ll 1$ and $g(A, x)$ is a bounded function of its arguments. As to the kinetic term $F(A)$, we shall assume that the autonomous ODE system

$$\dot{A} = F(A), \tag{157}$$

has a stable time-periodic solution $B(t) = B(t + P)$ for some $P > 0$. We now introduce a slow-time scale $T = \varepsilon t$, and look for solutions of (156) of the form

$$A(\varepsilon, t, x) = A^0(t, T, x) + \varepsilon A^1(t, T, x) + \varepsilon^2 A^2(t, T, x) + \cdots$$

requiring $A^1, A^2, \ldots$ to be bounded in time. Substituting this expansion into (156) gives

$$\frac{\partial A^0}{\partial t} = F(A^0), \tag{158}$$

$$\frac{\partial A^1}{\partial t} - \frac{\partial F}{\partial A}(A^0)A^1 = -\frac{\partial A^0}{\partial T} + D\Delta A^0 + g(x, A^0). \tag{159}$$

Solving (158) yields

$$A^0 = B(t + \psi(T, x)), \tag{160}$$

where $\psi(T, x)$ is a phase variable which remains undetermined at this stage. As a matter of fact, plugging (160) into (159), and looking then for bounded solutions in the resulting equation (which requires imposing a suitable orthogonality condition there), one eventually obtains that ψ satisfies

$$\frac{\partial \psi}{\partial T} = D_1(\Delta\psi + \Gamma|\nabla\psi|^2) + \alpha(x), \tag{161}$$

where

$$D_1 = \frac{1}{P}\int_0^P z^{\mathrm{T}}(s) D B'(s)\,\mathrm{d}s,$$

$$\Gamma = \frac{1}{P}\int_0^P z^{\mathrm{T}}(s) D B''(s)\,\mathrm{d}s, \tag{162}$$

$$\alpha(x) = \frac{1}{P}\int_0^P z^{\mathrm{T}}(s) g\big(x, B(s)\big)\,\mathrm{d}s,$$

and the vector z^{T} is periodic with period P and such that

$$\frac{\partial z^{\mathrm{T}}}{\partial t} + z^{\mathrm{T}} F_A\big(B(t+\psi)\big) = 0, \qquad z^{\mathrm{T}}(t+\psi)B'(t+\psi) = 1,$$

$$\int_0^P z^{\mathrm{T}} G\,\mathrm{d}s = 0,$$

where

$$G \equiv G(\psi, x, t) = -B'\frac{\partial \psi}{\partial T} + D\big(B'\Delta\psi + B''|\nabla\psi|^2\big) + g(x, B).$$

Summing up, we have obtained a solution of (156) in the form

$$A(x,t) = B\big(t + \psi(T,x)\big) + \mathrm{O}(\varepsilon), \tag{163}$$

where ψ solves (161). This representation is consistent with our assumption of a distributed medium consisting in a large population of individual oscillators, weakly coupled by diffusion, which produces a phase shift between different points, whose time evolution is described by (161).

It remains to be seen if (163) provides target patterns for (156). A remarkable fact is that this may be the case only if $g(x, A) \neq 0$, so that inhomogeneities in the medium are crucial for the onset of such type of waves in systems as (156). To check this statement, assume on the contrary that $g(x, A) = 0$. Then, by (162), $\alpha(x) = 0$ and setting $Z = \mathrm{e}^{\Gamma\psi}$, (161) reduces to

$$\frac{\partial Z}{\partial T} = D\Delta Z.$$

It then turns out that the initial value problem for (161) can be explicitly solved, and there holds

$$\psi(T,x) = \frac{1}{\Gamma}\log\left((4\pi D_1 T)^{-1}\int_{\mathbb{R}^2}\exp\left(\frac{\Gamma\psi(0,y) - |x-y|^2}{4D_1 T}\right)\mathrm{d}y\right).$$

From this formula we see that, if $\psi(0,x)$ is bounded, then $\psi(T,x)$ converges to a constant as $T \to \infty$, so that asymptotically the medium oscillates with uniform phase shift. When inhomogeneities are present, however, an asymptotic analysis detailed in [42] shows the existence of target patterns for (156), for which the propagation parameters are estimated.

As a next step, we now remark on the cocxistence of excitable and oscillatory regimes. This we shall do by following the arguments by Hagan and Cohen in [44]. In that work, a dynamical model for regulation of cAMP in *Dictyostelium discoideum* was proposed in terms of a number of variables: external (respectively internal) cAMP, cAMPe (respectively cAMPi), a cAMP inhibitor and a lump variable accounting for intracellular stored reserves. After performing a suitable asymptotic analysis, made possible by the separation of scales in the model that followed from the consideration of some small parameters, one is essentially led to analyziug the following system:

$$\dot{A} = f(A, C), \tag{164}$$

$$\dot{C} = k(A)S - h_1(C) \equiv g(A, C, S), \tag{165}$$

$$\dot{S} = \varepsilon\big(h_2(c) - k(A)S\big), \tag{166}$$

where $0 < \varepsilon \ll 1$, and f, k, h_1, h_2 are bounded functions whose qualitative behavior is depicted in Figure 7. As a matter of fact, small diffusivity effects are considered in [44]

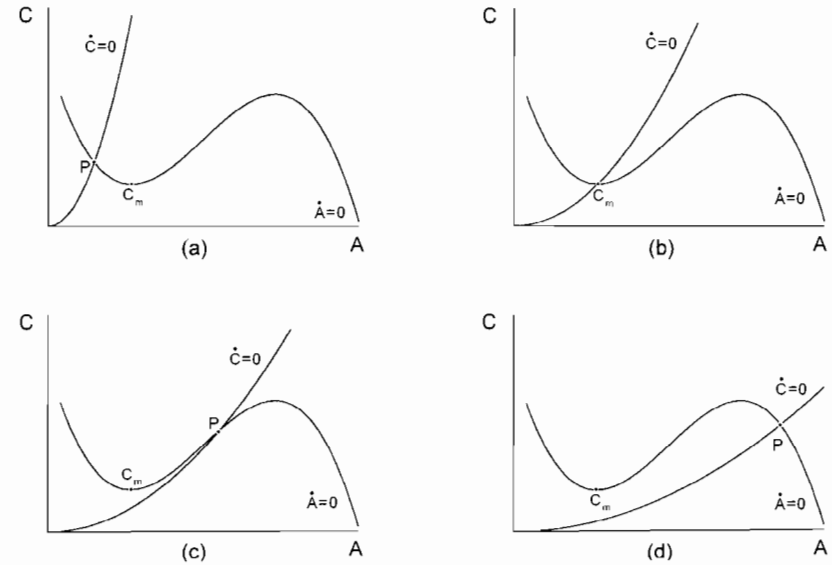

Fig. 7. Sequence of propagation regimes in system (164)–(167): (a) As P approaches C_m, excitability shows in, and cAMP pulses will propagate if triggered by a sufficiently large stimulus; (b) and (c) A Hopf bifurcation signals the entrance in the oscillatory regime. Region (d) corresponds to a stable equilibrium with high rates of synthesis and leakage of A. (Adapted from [44].)

(and should therefore be added to (164)–(166)), but these may be omitted in the forthcoming discussion. For completeness, we point out that variables A, C and S represent scaled versions of the intracellular cAMP, inhibitor and stored reserve concentrations respectively.

In (164)–(166), S can be thought of as a slowly varying parameter in the two-dimensional system consisting of (164) and (165), and its effect results in changes in the nullcline $g(A, C, S) = 0$ in (165). In this way, as S decreases the corresponding phase portrait goes from stages (a)–(d) in Figure 7.

At this juncture, the reader may wonder if one could possibly derive a multiscale model that should be able to account for individual behavior (including periodic firing at some pacemakers) on the one hand, and at the same time reproduce the transition and coexistence of macroscopic patterns as targets and spirals at the other extreme. At some stage, any such model is likely to involve an effective medium (or homogenization) approach. While no such model seems to be available as yet (cf. in this sense the discussion in [48]), it might be of some interest to shortly remark on the point of view recently developed in [101]. In that work, experiments on *Dd* mutant and wild-type (WT) strains are reported. A remarkable fact is that both mutant and WT cultures display optical density oscillations, although at a different pace in each case. In particular, the ability of mutant strains to produce self-organizing spiral patterns is seriously diminished, although the oscillation kinetics in all strains seem to be quite similar. A quantitative discussion on the spiral patterning is provided in [101], supplementary material. In doing so, the authors made use of a model system given by

$$\frac{\partial C}{\partial t} = D\Delta C - \Gamma C + H(C - C_{\mathrm{T}})C_{\mathrm{r}}, \tag{167}$$

$$C_{\mathrm{T}} = \left(C_{\max} - \frac{At}{t+T}\right)(1-E), \tag{168}$$

$$\frac{\partial E}{\partial t} = \eta + \beta C. \tag{169}$$

Here $C = C(x, y, t)$ stands for the concentration of *Dd* amoebae, which are assumed to be in one of three possible states: excitable, excited and refractory. When excitable cells are subject to a cAMP concentration exceeding a value C_{T}, they become excited and release a cAMP pulse C_{r}. After that, cells enter into a refractory state where no cAMP is secreted. In that period, C_{T} decreases from a value $C_{\max}$ to a value $C_{\min} < C_{\max}$ after a time $t = \tau > 0$ when they enter again into the excitable state. Excitability is represented in (167)–(169) by variable E; D, T, A, η, β are various positive parameters, and $H(s)$ is Heaviside function: $H(s) = 1$ if $s > 0$, $H(s) = 0$ otherwise. In particular, it was observed in [101] that when $\beta < 10^{-3}$ (low excitability) multiple firing centers appear, whereas for $\beta > 10^{-2}$ (high excitability) spiral waves are observed to persist. An interesting question would be to derive the evolution in time of β from data corresponding to interaction of *Dd* cells at the microscopic level.

Acknowledgements

This work has been supported by European Contract MRTN-CT-2004-503661 and by Acción Especial AE5/06-14364 from Universidad Complutense.

References

[1] T. Alarcón and K.M. Page, *Stochastic models of receptor oligomerization by bivalent ligand*, J. Roc. Soc. Interface (2006), published online, DOI: 10.1098/rsif: 2006.0116.
[2] T. Alarcón and K.M. Page, *Stochastic models of the VGEF receptor: Analysis and implications on anti-VGEF cancer therapy*, J. Roc. Soc. Interface (2006), submitted.
[3] R. Albert, Y.W. Chiu and H.G. Othmer, *Dynamic receptor team formation can explain the high signal transduction gain in Escherichia coli*, Biophysical J. **86** (2004), 2650–2659.
[4] D. Ambrosi, A. Gamba, E. Giraudo, G. Serini, L. Preziosi and F. Bussolino, *Burgers dynamics governs the early stages of vascular network assembly*, EMBO J. **22** (2003), 1771–1779.
[5] H. Baier and F. Bonhoeffer, *Axon guidance by gradients of a target-derived component*, Science **255** (1992), 472–475.
[6] N. Barkai and S. Leibler, *Robustness in simple biochemical networks*, Nature **387** (1997), 913–917.
[7] N. Bellomo, A. Bellouquid and M. Delitala, *Mathematical topics on the modeling of multicellular systems in the competition between tumor and immune cells*, Math. Models Methods Appl. Sci. **14** (2004), 1683–1733.
[8] N. Bellomo, A. Bellouquid and M.A. Herrero, *From microscopic to macroscopic description of multicellular systems and biological growing tissues*, Math. Cont. Mech., to appear.
[9] H.C. Berg, *Random Walks in Biology*, Princeton Univ. Press, Princeton, NJ, USA (1993).
[10] H.C. Berg, *E-coli in Motion*, Springer-Verlag, New York, USA (2003).
[11] H.C. Berg and E.M. Purcell, *Physics of chemoreception*, Biophysical Journal **20** (1977), 193–219.
[12] P. Biler, *Local and global solvability of some parabolic systems modeling chemotaxis*, Adv. Math. Sci. Appl. **9** (1998), 347–359.
[13] P. Biler, G. Karch, Ph. Laurençot and T. Nadzieja, *The 8π-problem for radially symmetric solutions of a chemotaxis model in the plane*, Preprint (2006).
[14] P. Biler, G. Karch, Ph. Laurençot and T. Nadzieja, *The 8π-problem for radially symmetric solutions of a chemotaxis model in a disc*, Preprint (2006).
[15] J.T. Bonner, *The Cellular Slime Mold*, Princeton Univ. Press, Princeton, NJ, USA (1967).
[16] J.T. Bonner, *Sixty Years of Biology*, Princeton Univ. Press, Princeton, NJ, USA (1996).
[17] D. Bray, M.D. Levin and C.J. Morton-Firth, *Receptor clustering as a cellular mechanism to control sensitivity*, Nature **393** (1998), 85–88.
[18] F.A. Chalub, P. Markowich, B. Perthame and C. Schmeiser, *Kinetic models for chemotaxis and their drift-diffusion limits*, Monatsh. Math. **142** (2004), 123–141.
[19] S. Chandrasekhar, *Stochastic problems in physics and astronomy*. Rev. Mod. Phys. **15** (1943), 1–91.
[20] N.B. Charvet, K. Brose, K. Wang, V. Marillat, T. Kidd, C.S. Goodman, M. Tessier-Lavigne, C. Sotelo and A. Chedotal, *Slit-2 mediated chemorepulsion and collapse of developing forebrain axons*, Neuron **22** (1999), 463–473.
[21] S. Childress, *Chemotactic collapse in two dimensions*, Lecture Notes in Biomathematics (Springer) **55** (1984), 61–66.
[22] S. Childress and J.K. Percus, *Nonlinear aspects of chemotaxis*, Math. Biosci. **56** (1981), 217–237.
[23] R.L. Chisholm and R.A. Firtel, *Insights into morphogenesis from a simple developmental system*, Nature Rev. Mol. Cell Biol. **5** (2004), 531–541.
[24] L. Corrias, B. Perthame and H. Zaag, *Global solutions of some chemotaxis and angiogenesis systems in high space dimensions*, Milan J. Math. **72** (2004), 1–28.
[25] J. Crank, *The Mathematics of Diffusion*, Oxford Univ. Press, Oxford, UK (2003).
[26] J.C. Dallon and H.G. Othmer, *A continuum analysis of the chemotactic signal seen by Dictyostelium discoideum*, J. Theoret. Biol. **194** (1998), 461–483.

[27] F. de Castro, *Chemotropic molecules: Guides for axonal pathfinding and cell migration during CNS development*, News Physiol. Sci. **18** (2003), 130–136.
[28] C. De Lisi, F. Marchetti and G. Del Grosso, *A theory for measurement error and its implications for spatial and temporal gradient sensing during chemotaxis*, Cell Biophys. **4** (1982), 211–229.
[29] C. De Lisi, and F. Marchetti, *A theory for measurement error and its implications for spatial and temporal gradient sensing during chemotaxis, II: The effects of non-equilibrated ligand binding*, Cell Biophys. **5** (1983), 237–253.
[30] A. Deutsch and S. Dormann, *Cellular Automaton Modeling of Biological Pattern Formation*, Birkhäuser, Boston, MA, USA (2005).
[31] M. Eisenbach, ed., *Chemotaxis*, Imperial College Press, London, UK (2004).
[32] R. Erban and H.G. Othmer, *From individual to collective behaviour in bacterial chemotaxis*, SIAM J. Appl. Math. **65** (2004), 361–391.
[33] R. Erban and H.G. Othmer, *From signal transduction to spatial pattern formation in E. coli: A paradigm for multi-scale modeling in biology*, Multiscale Model. Simul. **3** (2) (2005), 362–394.
[34] R. Escalante and J.J. Vicente, *Dictyostelium discoideum: A model system for differentiation and patterning*, Int. J. Devel. Biol. **44** (2000), 819–835.
[35] B. Fiedler and A. Scheel, *Spatio-temporal dynamics of reaction–diffusion patterns*, Trends in Nonlinear Analysis, Springer-Verlag, Berlin (2002), 21–150.
[36] S.K. Friedlander, *Smoke, Dust and Haze: Fundamentals of Aerosol Dynamics*, Oxford Univ. Press, New York, USA (2000).
[37] A. Gamba, D. Ambrosi, A. Coniglio, A. de Candia, S. DiTalia, E. Giraudo, G. Serini, L. Preziosi and F. Bussolino, *Percolation, morphogenesis and Burgers dynamics in blood vessels formation*, Phys. Rev. Lett. **90** (2003), 11810–11814.
[38] C.W. Gardiner, *Handbook of Stochastic Methods for Physics, Chemistry and the Natural Sciences*, Springer-Verlag (1997).
[39] A. Gierer and H. Meinhardt, *A theory of biological pattern formation*, Kybernetik **12** (1972), 30–39.
[40] G.J. Goodhill and J.S. Urbach, *Theoretical analysis of gradient detection by growth cones*, J. Neurobiol. **41** (1999), 230–241.
[41] R. Gordon and L. Beloussov, *From observations to paradigms: The importance of theories and models. An interview with Hans Meinhardt*, Int. J. Devel. Biol. **50** (2006), 103–111.
[42] P.S. Hagan, *Target patterns in reaction–diffusion systems*, Adv. in Appl. Math. **42** (1981), 762–786.
[43] P.S. Hagan, *Spiral waves in reaction–diffusion equations*, SIAM J. Appl. Math. **42** (1982), 762–786.
[44] P.S. Hagan and M.S. Cohen, *Diffusion-induced morphogenesis in the development of Dictyostelium*, J. Theoret. Biol. **93** (1981), 881–908.
[45] R. Heinrich, B.G. Neel and T.A. Rapoport, *Mathematical models of protein kinase signal transduction*, Molecular Cell **9** (2002), 957–970.
[46] M.A. Herrero, *Reaction–diffusion systems: A mathematical biology approach*, Cancer Modelling and Simulations, L. Preziosi, ed., Chapman & Hall (2003), 367–420.
[47] M.A. Herrero, E. Medina and J.J.L. Velázquez, *Finite-time aggregation into a single point in a reaction–diffusion system*, Nonlinearity **10** (1997), 1754–1793.
[48] M.A. Herrero and L. Sastre, *Models of aggregation in Dictyostelium discoideum: On the track of spiral waves*, Networks and Heterogeneous Media **1** (2) (2006), 241–258.
[49] M.A. Herrero and J.J.L. Velázquez, *Chemotactic collapse for the Keller–Segel model*, J. Math. Biol. **35** (1996), 177–196.
[50] T. Hillen and H.G. Othmer, *The diffusion limit of transport equations derived from velocity-jump processes*, SIAM J. Appl. Math. **61** (3) (2000), 751–775.
[51] D. Horstmann, *From 1970 until present: The Keller–Segel model in chemotaxis and its consequences I*, Jahresber. Deutsch. Math.-Verein. **105** (3) (2003), 103–165.
[52] L.N. Howard and N. Koppel, *Slowly varying waves and shock structures in reaction–diffusion equations*, Stud. Appl. Math. **56** (1977), 95–145.
[53] P.A. Iglesias and A. Levchenko, *Modelling the cell's guidance system*, Science STKE, available at http://stke.sciencemag.org/cgi/content/full/sigtransj2002/148/ /rel2 (2002).
[54] W. Jäger and S. Luckhaus, *On explosions of solutions to a system of partial differential equations modeling chemotaxis*, Trans. Amer. Math. Soc. **239** (1992), 817–824.
[55] F. John, *Partial Differential Equations*, Appl. Math. Sci., Vol. 1, Springer-Verlag, New York, USA (1980).
[56] E.F. Keller, *Making Sense of Life: Explaining Biological Development with Models, Metaphors and Machines*, Harvard Univ. Press, Cambridge, MA, USA (2002).
[57] E.F. Keller and L.A. Segel, *Initiation of slime mold aggregation viewed as an instability*, J. Theoret. Biol. **26** (1970), 399–415.
[58] S.H. Kim, W. Wang and K.K. Kim, *Dynamic and clustering model of bacterial chemotaxis receptors: Structural basis for signaling and high sensitivity*, Proc. Natl. Acad. Sci. USA **99** (18) (2002), 11611–11615.
[59] T.M. Konijn, J.G.C. van de Meere, J.T. Bonner and D.S. Barkley, *The acrasin activity is adenosin – 3′,5′-cyclic phosphate*, Proc. Natl. Acad. Sci. USA **58** (1967), 1152–1154.
[60] R. Kowalczyk, *Preventing blow-up in a chemotaxis model*, J. Math. Anal. Appl. **305** (2005), 566–580.
[61] R. Kowalczyk, A. Gamba and L. Preziosi, *On the stability of homogeneous solutions to some aggregation models*, Discrete Contin. Dyn. Syst. (4) **13** (2004), 204–220.
[62] J. Krishnan, P.A. Iglesias and L. Ma, *Spatial sensing of chemotactic gradients: A reaction–diffusion model*. Proc. 2nd Internat. Conf. System Biology, Pasadena, CA (2001), 148–157.
[63] Y. Kuramoto, *Chemical Oscillations, Waves and Turbulence*, Springer-Verlag, Berlin (1984).
[64] Y. Kuramoto and S. Koga, *Turbulized rotating chemical waves*, Progr. Theoret. Phys. **66** (1981), 1081–1085.
[65] D.A. Lauffenburger and J.J. Linderman, *Receptors: Models for Binding, Trafficking and Signalling*. Oxford Univ. Press, Oxford, UK (1993).
[66] J. Lauzeral, J. Halloy and A. Goldbeter, *Desynchronization of cells on the developmental path triggers the formation of spiral waves of cAMP during Dictyostelium aggregation*, Proc. Natl. Acad. Sci. USA **94** (1997), 9153–9158.
[67] K.J. Lee, E.C. Cox and R.E. Goldstein, *Competing patterns of signalling activity in Dictyostelium discoideum*, Phys. Rev. Lett. **76** (7) (1996), 1174–1177.
[68] K.J. Lee, R.E. Goldstein and E.C. Cox, *Resetting wave forms in Dictyostelium territories*, Phys. Rev. Lett. **87** (6) (2001), 0681011.
[69] K.J. Lee, R.E. Goldstein and E.C. Cox, *cAMP waves in Dictyostelium territories*, Nonlinearity **15** (2002), C1–C5.
[70] A. Levchenko and P.A. Iglesias, *Models of eukaryotic gradient sensing: Application to chemotaxis of amoebae and neutrophils*, Biophys. J. **82** (2002), 50–63.
[71] M.D. Levin, T.S. Shimizu and D. Bray, *Binding and diffusion of CheR molecules within a cluster of membrane receptors*, Biophys. J. **82** (2002), 1809–1817.
[72] S. Luckhaus and Y. Sugiyama, *Asymptotic profile with the optimal convergence rate for a parabolic equation of chemotaxis in super-critical cases*, Preprint (2006).
[73] M. Maeda, *Regulation of growth and differentiation in Dictyostelium*, Int. Rev. Cytolog. **244** (2005), 287–332.
[74] J.L. Martiel and A. Goldbeter, *A model based on receptor desensitization for cyclic-AMP signalling in Dictyostelium cells*, Biophys. J. **52** (1987), 807–828.
[75] J.M. Mato, A. Losada, V. Nanjundiah and T.M. Konijn, *Signal input for a chemotactic response in the cellular slime mold Dictyostelium discoideum*, Proc. Natl. Acad. Sci. USA **72** (1975), 4991–4993.
[76] H. Meinhardt, *Models of Biological Pattern Formation*, Academic Press, Manchester, UK (1982).
[77] H. Meinhardt, *Orientation of chemotactic cells and growth cones: Models and mechanisms*, J. Cell Sci. **112** (1999), 2867–2874.
[78] H. Meinhardt, *Out-of-phase oscillations and traveling waves with unusual properties: The use of three-component systems in biology*, Physica D **199** (2003), 264–277.
[79] A.S. Mikhailov, *Foundations of Synergetics I*, Springer-Verlag, New York (1994).
[80] T. Nagai, *Blow-up of radially symmetric solutions to a chemotaxis system*, Adv. Math. Sci. Appl. **5** (1995), 1–21.
[81] T. Nagai, T. Senba and T. Suzuki, *Chemotaxis collapse in a parabolic system of mathematical biology*, Hiroshima Math. J. **30** (2000), 463–497.
[82] V. Nanjundiah, *Chemotaxis, signal relaying and aggregation morphology*, J. Theoret. Biol. **42** (1973), 63–105.

[83] H.G. Othmer, S.R. Dunbar and W. Alt, *Models of dispersal of biological populations*, J. Math. Biol. **26** (1998), 263–298.
[84] H.G. Othmer and T. Hillen, *The diffusion limit of transport equations, II: Chemotaxis equations*, SIAM J. Appl. Math. **62** (4) (2002), 1222–1250.
[85] H.G. Othmer and P. Schaap, *Oscillating signaling in the development of Dictyostelium discoideum*, Comments. Theor. Biol. **5** (1998), 175–282.
[86] H.G. Othmer and A. Stevens, *Aggregation, blow-up and collapse. The ABC's of generalized taxis*, SIAM J. Appl. Math. **57** (1997), 1044–1081.
[87] K.J. Painter and T. Hillen, *Volume-filling and quorum-sensing in models for chemosensitive movement*, Canad. Appl. Math. Quart. **10** (4) (2004), 501–543.
[88] E. Palsson and E.C. Cox, *Origin and evolution of circular waves and spirals in Dictyostelium discoideum territories*, Proc. Natl. Acad. Sci. USA **93** (1996), 1151–1155.
[89] A.S. Perelson, *Receptor clustering on a cell surface II. Theory of receptor cross-linking by ligands bearing two chemically distinct functional groups*, Math. Biosci. **49** (1980), 87–110.
[90] A.S. Perelson, *Receptor clustering on a cell surface, III. Theory of receptor cross-linking by multivalent ligands: Description of ligand states*, Math. Biosci. **53** (1981), 1–39.
[91] A.S. Perelson and C. De Lisi, *Receptor clustering on a cell surface I. Theory of receptor cross-linking by ligands bearing two chemically identical functional groups*, Math. Biosci. **48** (1980), 71–110.
[92] B. Perthame, *PDE models for chemotactic movements: Parabolic, hyperbolic and kinetics*, Appl. Math. **49** (2004), 539–564.
[93] R.G. Posner, C. Wofsy and B. Goldstein, *The kinetics of bivalent ligand-bivalent receptor aggregation: Ring formation and the breakdown of equivalent site approximation*, Math. Biosci. **126** (1995), 171–190.
[94] S. Ramón y Cajal, *La retine des vertébrés*, La Cellulle **9** (1893), 119–255.
[95] S. Ramón y Cajal, *Nouvelles observations sur l'evolution des neuroblastes avec quelques remarques sur l'hypothese neurogénétique de Hensen–Held*, Anat. Anzeiger Bd. XXXII (1908).
[96] S. Ramón y Cajal, *Estudios sobre la degeneración y regeneración del sistema nervioso*, Vols 1 and 2, Moya, Madrid (1913–1914).
[97] K.B. Raper, *Dictyostelium discoideum, a new species of slime mold from decaying forest leaves*, J. Agr. Res. **50** (1935), 135–147.
[98] W.J. Rappel, P.J. Thomas, H. Levine and W.F. Loomis, *Establishing direction during chemotaxis in eukaryotic cells*, Biophys. J. **83** (2002), 1361–1367.
[99] C. Roisin-Bouffey, W. Jang, D.R. Caprette and R.H. Gomer, *A precise group size in Dictyostelium is generated by a cell-counting factor modulating cell–cell adhesion*, Mol. Cell **6** (2000), 953–959.
[100] P.G. Saffman and M. Delbrück, *Brownian motion in biological membranes*, Proc. Natl. Acad. Sci. USA **72** (8) (1975), 3111–3113.
[101] S. Sawal, P.A. Thomson and E.C. Cox, *An autoregulatory circuit for long-range self-organization in Dictyostelium cell populations*, Nature **433** (2005), 323–326.
[102] A. Scheel, *Bifurcation to spiral waves in reaction–diffusion systems*, SIAM J. Math. Anal. **29** (1998), 1399 1418.
[103] J.E. Segall, S.M. Block and H.C. Berg, *Temporal comparisons in bacterial chemotaxis*, Proc. Natl. Acad. Sci. USA **83** (1986), 8987–8991.
[104] T. Serafini, T.E. Kennedy, M.J. Galko, C. Mirzayan, T.M. Jessell and M. Tessier-Lavigne, *The neutrins define a family of axon outgrowth-promoting proteins homologous to C. elegans UNC–6*, Cell **78** (1994), 409–424.
[105] C. Sotelo, *The chemotactic hypothesis of Cajal: A century behind*, Progr. Brain Res. **136** (2002), 11–20.
[106] V. Sourjik and H.C. Berg, *Receptor sensitivity in bacterial chemotaxis*, Proc. Natl. Acad. Sci. USA **99** (2002), 123–127.
[107] P. Spiro, J.S. Parkinson and H.G. Othmer, *A model of excitation and adaptation in bacterial chemotaxis*, Proc. Natl. Acad. Sci. USA **94** (1997), 7263–7268.
[108] A. Stevens, *Derivation of chemotaxis equations as limit dynamics of moderately interacting stochastic many particle systems*, SIAM J. Appl. Math. **61** (1) (2000), 183–212.
[109] Y. Sugiyama, *Global existence in sub-critical cases and finite time blow-up in supercritical cases to degenerate Keller–Segel systems*, J. Differential Equations (2006), to appear.

[110] Y. Sugiyama and H. Kunii, *Global existence and decay properties for a degenerate Keller–Segel model with a power factor in drift term*, J. Differential Equations (2006), to appear.
[111] T. Suzuki, *Free-energy and self-interacting particles*, Progr. Nonlinear Differential Equations, Vol. 62, Birkhäuser, Boston, USA (2005).
[112] Y. Tang and H.G. Othmer, *Excitation, oscillations and wave propagation in a G-protein based model of signal transduction in Dictyostelium discoideum*, Philos. Trans. Roy. Soc. London Ser. B **349** (1995), 179–195.
[113] M. Tessier-Lavigne, M. Placzek, A.G. Lumsden, J. Dodd and T.M. Jessell, *Chemotropic guidance of developing axons in the mammalian central nervous system*, Nature **336** (1988), 75–778.
[114] A.M. Turing, *The chemical basis of morphogenesis*, Philos. Trans. Roy. Soc. London **237** (1952), 37–72.
[115] P.J.M. van Haastert and P.N. Devreotes, *Chemotaxis: Signalling the way forward*, Nature Rev. Mol. Cell Biol. **5** (2004), 626–634.
[116] A. van Oojen, *Modeling Neural Development*, MIT Press, Cambridge, MA, USA (2003).
[117] J.J.L. Velázquez, *Point dynamics in a singular limit of the Keller–Segel model, I. Motion of the concentration regions*, SIAM J. Appl. Math. **64** (4) (2004), 1198–1223.
[118] J.J.L. Velázquez, *Point dynamics in a singular limit of the Keller–Segel model, II. Formation of the concentration regions*, SIAM J. Appl. Math. **64** (4) (2004), 1224–1248.
[119] D. Wzrosek, *Global attractor for a chemotaxis model with prevention of overcrowding*, Preprint (2004).
[120] T.M. Yi, Y. Huang, M.L. Simon and J. Doyle, *Robust perfect adaptation in bacterial chemotaxis through integral feedback control*, Proc. Natl. Acad. Sci. USA **97** (9) (2000), 4649–4653.
[121] S.H. Zigmond, *Ability of polymorphonuclear leukocytes to orient in gradients of chemotactic factors*, J. Cell. Biol. **75** (1977), 606–616.
[122] R. Zwanzig, *Diffusion-controlled ligand binding to spheres partially covered by receptors: An effective medium treatment*, Proc. Natl. Acad. Sci. USA **87** (1990), 5856–5857.